



HAL
open science

Titan's cloud seasonal activity from winter to spring with Cassini/VIMS

Sebastien Rodriguez, Stéphane Le Mouélic, Pascal Rannou, Christophe Sotin,
Robert Brown, Jason Barnes, Caitlin Griffith, Jérémie Buralat, Kevin
Baines, Bonnie Buratti, et al.

► **To cite this version:**

Sebastien Rodriguez, Stéphane Le Mouélic, Pascal Rannou, Christophe Sotin, Robert Brown, et al..
Titan's cloud seasonal activity from winter to spring with Cassini/VIMS. *Icarus*, 2011, 216, pp.89 -
110. 10.1016/j.icarus.2011.07.031 . hal-03657788

HAL Id: hal-03657788

<https://hal.science/hal-03657788>

Submitted on 3 May 2022

HAL is a multi-disciplinary open access archive for the deposit and dissemination of scientific research documents, whether they are published or not. The documents may come from teaching and research institutions in France or abroad, or from public or private research centers.

L'archive ouverte pluridisciplinaire **HAL**, est destinée au dépôt et à la diffusion de documents scientifiques de niveau recherche, publiés ou non, émanant des établissements d'enseignement et de recherche français ou étrangers, des laboratoires publics ou privés.

Manuscript Number: ICARUS-11663R3

Title: Titan's cloud seasonal activity from winter to spring with Cassini/VIMS

Article Type: Regular Article

Keywords: Satellites, atmosphere; Titan; Titan, atmosphere; Titan, clouds; Meteorology

Corresponding Author: Dr Sebastien Rodriguez,

Corresponding Author's Institution: Laboratoire AIM - Universite Paris Diderot

First Author: Sebastien Rodriguez

Order of Authors: Sebastien Rodriguez; Stephane Le Mouelic; Pascal Rannou; Christophe Sotin; Robert H Brown; Jason W Barnes; Caitlin A Griffith; Jerome Buralat; Kevin H Baines; Bonnie J Buratti; Roger N Clark; Phil D Nicholson

Abstract: Since Saturn orbital insertion in July 2004, the Cassini orbiter has been observing Titan throughout most of the northern winter season (October 2002-August 2009) and the beginning of spring, allowing a detailed monitoring of its cloud coverage at high spatial resolution with Titan's close flybys on a monthly basis. This study reports on the analysis of all the near-infrared images of Titan's clouds acquired by the Visual and Infrared Mapping Spectrometer (VIMS) during 67 targeted flybys of Titan between July 2004 and April 2010.

The VIMS observations show numerous sporadic clouds at southern high and mid-latitudes, rare clouds in the equatorial region, and reveal a long-lived cloud cap above the north pole, ubiquitous poleward of 60°N. These observations allow us to follow the evolution of the cloud coverage during almost a six-year period including the equinox, and greatly help to further constrain global circulation models (GCMs). After four years of regular outbursts observed by Cassini between 2004 and 2008, southern polar cloud activity started declining, and completely ceased one year before spring equinox. The extensive cloud system over the north pole, stable between 2004 and 2008, progressively fractionated and vanished as Titan entered into northern spring. At southern mid-latitudes, clouds were continuously observed throughout the VIMS observing period, even after equinox, in a latitude band between 30°S and 60°S. During the whole period of observation, only a dozen clouds were observed closer to the equator, though they were slightly more frequent as equinox approached. We also investigated the distribution of clouds with longitude. We found that southern polar clouds, before disappearing in mid-2008, were systematically concentrated in the leading hemisphere of Titan, in particular above and to the east of Ontario Lacus, the largest reservoir of hydrocarbons in the area. Clouds are also non-homogeneously distributed with longitude at southern mid-latitudes. The n=2-mode wave pattern of the distribution, observed since 2003 by Earth-based telescopes and confirmed by our Cassini observations, may be attributed to Saturn's tides.

Although the latitudinal distribution of clouds is now relatively well reproduced and understood by the GCMs, the non-homogeneous longitudinal distributions and the evolution of the cloud coverage with seasons still need investigation. If the observation of a few single clouds at the tropics and at northern mid-latitudes late in winter and at the start of spring cannot be further interpreted for the moment, the obvious shutdown of the cloud activity at Titan's poles provides clear signs of the onset of the general circulation turnover that is expected to accompany the beginning of Titan's northern spring. According to our GCM, the persistence of clouds at certain latitudes rather suggests a 'sudden' shift in near future

of the meteorology into the more illuminated hemisphere. Finally, the observed seasonal change in cloud activity occurred with a significant time lag that is not predicted by our model. This may be due to an overall methane humidity at Titan's surface higher than previously expected.

*Highlights

- An extensive and stable cloud caps the pole during winter.
- Transient, convective clouds form in the summer hemisphere at preferential latitudes.
- At summer pole clouds form preferably above the largest liquid reservoir available.
- Saturn's tides may shape the cloud distribution over longitudes.
- When winter ends, clouds vanish at both poles, sign of the onset of circulation turnover.

Point by point response to issues raised by reviewer #2 (3rd round of review)

**Paper entitled 'Titan's cloud activity from winter to spring with Cassini/VIMS'
by Rodriguez et al. (Manuscript #ICARUS-11663R2)**

Below is a response to the points raised by Reviewer #2 in the mail sent by Andrew P. Ingersoll on Friday 8 July 2011. The reviewer's comments are in black plain text and our response in blue.

Reviewer's comments:

Reviewer #2: The paper is greatly improved and clarified by the inclusion of separate low methane and ethane cloud and high ethane cloud maps. The discussion of the cloud predictions and comparison with GCM results (pages 20 - 24) are fine now, apart from a few points noted below:

(1) To me, a significant result in terms of the comparison between GCMs and observations is that both GCMs predict a gap in cloud activity between $\sim 50^\circ$ and 60° or 65° S, which is also found in observations when you look at the fractional cloud detection as in e.g. Figure 2d. It is far less obvious from e.g. Figure 3, where there appears to be almost as much cloud activity in this region as at lower latitudes [presumably because Figure 3 focuses on timing and latitudinal coverage rather than longitudinal coverage or persistence]. This result seems to get slightly lost in the paper as it stands.

After "Neither of the two models produces significant cloud cover/condensation at $65-85^\circ$ S where most of the numerous convective polar clouds are observed." (lines 475-477), we have added the following sentence: "Nevertheless, the gap in cloud activity between $\sim 50^\circ$ and 65° S is well predicted by both GCMs."

(2) Lines 530-532: "In the same way, our recent observations continue to show no sign for a gradual vanishing of the $\sim 40^\circ$ S cloud activity, predicted by the IPSL-TGCM to occur starting in mid-2007." The sentence before this discussed a prediction of polar clouds ceasing that occurs later in observations, but in the case of the 40S cloud activity vanishing it has not been established in the paper that this will happen at all, so I query starting this sentence with the words "In the same way". Also, if the time lag were the same as for the southern polar clouds, these clouds should have started to disappear in mid-2010 (after which you show no observations, so you can't tell either way). So I think the words "in the same way" are misleading and would suggest rephrasing this sentence. E.g. "Our recent observations do not yet show the $\sim 40^\circ$ s cloud activity disappearing, as predicted by the IPSL-TGCM to occur starting in mid-2007, though it is still possible that this will occur following a time lag."

This sentence has been reworded as advised by the reviewer.

Note: I completely understand that you don't want to extend the full study for this paper, but given that it is now mid-2011, it seems odd to claim no knowledge of whether the 40S cloud activity disappeared by mid-2010 or not.

Surely this is known by now? If cloud activity has ceased, this supports your claim that you are predicting Titan well with a constant time lag, but if cloud activity has not ceased you should note that - while cloud activity may still cease at some later time - the time lag (between observations and model) will be greater than for the polar clouds.

(3) Lines 570-573: "GCMs generally predict large scale circulation and may miss local, but strong circulation able to produce ascending motion and clouds. This could also explain the more frequent occurrence of clouds near the equator as Titan is going through and beyond equinox." But surely the passage of the upward branch of Hadley cell across the equator in the equinoctial season explains near-equatorial clouds? Or does the timing and/or cloud location not synchronize with this idea? It just seems strange to specifically mention a region and time when one might expect the effect of the Hadley cell upward branch to be greater than local scale circulations.

This is true only if the ITCZ follow the latitude of the maximum of insolation with no lag. If the ITCZ stays blocked at mid-latitudes during summer, as predicted by the IPSL-TGCM, then one of the possibilities to produce cloud activity at tropics come from the local scale circulation. The idea of an ITCZ locked at 40° of latitude during the whole summer is strongly supported by our observations of persistent 40°S clouds, even after equinox.

We have changed the second sentence as follow: "If we consider that the ITCZ stays locked at summer mid-latitudes (Rannou et al., 2006), as suggested by the invariable observation of clouds at $\sim 40^\circ\text{S}$, local scale circulations could explain the more frequent occurrence of clouds near the equator, as Titan is going through and beyond equinox and tropics are more and more powered by solar illumination."

(4) Lines 581, 582: "the persistence of clouds at 40°S through mid-2010. clearly indicates the onset of the circulation turnover and seems to imply an 'abrupt' hemispherical reversal of cloud activity" - I was confused about how clouds persisting (when the model predicted they would cease) could be used to imply an abrupt change. However, I think the authors are saying that if the transition is more gradual (as in Mitchell's work) then they would have expected to see the cloud latitude shifting.

Is that correct? If so, this may need clarification. [I.e., clarifying that it is the roughly constant latitude of the persistent clouds that supports this argument, rather than the fact that they persist.]

Reviewer is right here. We have clarified this point by rewording the sentence: "2) the constant appearance of clouds at 40°S through mid-2010".

(5) Lines 1132-1138: This paragraph discusses errors in Brown et al. [2010], but I believe the authors intended to reference Brown et al.'s Figure 6 rather than Figure 7. I suggest referencing e.g. Barnes et al. [2009] here as well as Table 1 for the 'correct' flybys. This is indeed Figure 6 from Brown et al. (2010). This has been corrected. We now reference Table 1 from Barnes et al. (2009) in the caption of our Table A1, even if they only deal with the Cassini nominal mission (up to July 2008).

Note: The authors note that Brown et al. omitted 2 flybys from their Figure, and also erroneously shifted a number of them by six months. I attempted to check this but actually found it extremely difficult to figure out what was going on in the Brown et al. figure (aside from it clearly having errors). Short of writing my own code to plot, skip and shift flyby dates, I will have to trust that the authors have done a more careful analysis and are confident in their conclusions about what went wrong with the Brown et al. figure. Basically, though, I agree that it was wrong, and the authors' suggested errors seem plausible.

We agree that such errors can only be detected by persons doing the hard work to carefully check all the dataset in detail, as we did for this paper. Here, we report errors, and we know that people must either trust us, or check our statements by doing the checking themselves (we give here all the information to check again the dataset).

Minor changes:

(a) Line 436: "On its side, the IPSL" -> "The IPSL" - 'on its side' reads poorly, and also may suggest an odd geometry for the model ;)

Done.

(b) Lines 484-485 "Already stated in Rodriguez et al. (2009), the erroneous prediction of the ~40°N clouds by the IPSL-TGCM during the southern summer allows to put a diagnostic on the failure of the model". I think "allows to put a diagnostic on" is the wrong phrasing (and doesn't actually make sense). Something simpler, such as ".southern summer is a failure of the model" would be better. Also "Already stated in" should be "As stated in".

Done.

(c) Lines 529, 530: brings another evidence -> provides more evidence

Done.

(d) Lines 538, 539: the persistence of a convective activity -> the persistence of convective activity

Done.

(e) Line 561: related with -> related to

Done.

(f) Line 571: both "circulation" -> "circulations"

Done.

(g) Lines 574, 575: as strong degassing from the ground -> such as strong degassing from the ground

Done.

(h) Line 580: the cease of -> the cessation of

Done.

(i) Line 818: "efficient" seems an odd choice here - is it truly more efficient or is it "required."

The sentence has been changed as follow: "A fully 3D model may be also required to predict with more efficiency the haze and cloud microphysics and the seasonality of Titan's clouds and/or precipitation."

(j) Line 1091: We thus realized -> We thus performed [?]

Done.

(k) Line 1120: "In counterpart it appears to be" - doesn't read well - shouldn't this be something like e.g. "At the same time it appears to be" ?

Done.

(l) Lines 1140,1141: "has the advantage to produce reproducible results taking the same dataset, algorithm and criteria of detection." I suggest e.g. "has the advantaging of producing identical results every time, given the same dataset and detection criteria."

Done.

(m) Line 1177: "The latitude coverage of Titan's with time" - of Titan's what? Should this have been "The latitudinal coverage of Titan's cloud activity with time" ?

Done.

34 **Abstract**

35

36 Since Saturn orbital insertion in July 2004, the Cassini orbiter has been observing Titan
37 throughout most of the northern winter season (October 2002-August 2009) and the beginning
38 of spring, allowing a detailed monitoring of its cloud coverage at high spatial resolution with
39 Titan's close flybys on a monthly basis. This study reports on the analysis of all the near-
40 infrared images of Titan's clouds acquired by the Visual and Infrared Mapping Spectrometer
41 (VIMS) during 67 targeted flybys of Titan between July 2004 and April 2010.

42 The VIMS observations show numerous sporadic clouds at southern high and mid-latitudes,
43 rare clouds in the equatorial region, and reveal a long-lived cloud cap above the north pole,
44 ubiquitous poleward of 60°N. These observations allow us to follow the evolution of the
45 cloud coverage during almost a six-year period including the equinox, and greatly help to
46 further constrain global circulation models (GCMs). After four years of regular outbursts
47 observed by Cassini between 2004 and 2008, southern polar cloud activity started declining,
48 and completely ceased one year before spring equinox. The extensive cloud system over the
49 north pole, stable between 2004 and 2008, progressively fractionated and vanished as Titan
50 entered into northern spring. At southern mid-latitudes, clouds were continuously observed
51 throughout the VIMS observing period, even after equinox, in a latitude band between 30°S
52 and 60°S. During the whole period of observation, only a dozen clouds were observed closer
53 to the equator, though they were slightly more frequent as equinox approached.

54 We also investigated the distribution of clouds with longitude. We found that southern polar
55 clouds, before disappearing in mid-2008, were systematically concentrated in the leading
56 hemisphere of Titan, in particular above and to the east of Ontario Lacus, the largest reservoir
57 of hydrocarbons in the area. Clouds are also non-homogeneously distributed with longitude at
58 southern mid-latitudes. The n=2-mode wave pattern of the distribution, observed since 2003

59 by Earth-based telescopes and confirmed by our Cassini observations, may be attributed to
60 Saturn's tides.

61 Although the latitudinal distribution of clouds is now relatively well reproduced and
62 understood by the GCMs, the non-homogeneous longitudinal distributions and the evolution
63 of the cloud coverage with seasons still need investigation. If the observation of a few single
64 clouds at the tropics and at northern mid-latitudes late in winter and at the start of spring
65 cannot be further interpreted for the moment, the obvious shutdown of the cloud activity at
66 Titan's poles provides clear signs of the onset of the general circulation turnover that is
67 expected to accompany the beginning of Titan's northern spring. According to our GCM, the
68 persistence of clouds at certain latitudes rather suggests a 'sudden' shift in near future of the
69 meteorology into the more illuminated hemisphere. Finally, the observed seasonal change in
70 cloud activity occurred with a significant time lag that is not predicted by our model. This
71 may be due to an overall methane humidity at Titan's surface higher than previously
72 expected.

73

74 *Keywords:* Satellites, atmosphere; Titan; Titan, atmosphere; Titan, clouds; Meteorology

75

76 **1. Introduction**

77

78 Titan is the only moon in the solar system with a dense atmosphere. Its atmospheric
79 dynamics are driven by latitudinal temperature differences and seasonal temperature
80 variations. Saturn has an inclination of 26° relative to its orbital plane. This largest satellite of
81 Saturn has a near-equatorial orbit and, like Saturn, has seasons about 30 times longer than
82 those on Earth. During northern winter, the south pole is always illuminated whereas the north
83 pole is not, resulting in a temperature difference generating an atmospheric circulation
84 globally from the southern hemisphere to the northern hemisphere. The circulation takes the
85 form of a Hadley cell in the troposphere, which most of the time has an ascending branch near
86 30-40° in the summer hemisphere, subsiding near the polar regions (Tokano et al., 2001;
87 Tokano, 2005; Rannou et al., 2006; Mitchell et al., 2006, 2009). In the stratosphere, the
88 circulation takes the form of a single direct cell with a broad ascending branch in the summer
89 hemisphere and a descending branch well confined in the winter polar region.

90 Titan's nitrogen-laden atmosphere contains the trace condensable gas methane with a
91 mixing ratio of about 1.65% overall, but increasing to 5% close to the surface at the Huygens
92 landing site (Fulchignoni et al., 2005; Tomasko et al., 2005), where conditions are close to the
93 methane triple point. This situation is similar to that of H₂O on Earth, with liquid methane
94 possibly filling the lakes imaged by the RADAR instrument (Stofan et al., 2007). Flows of
95 liquid methane are also thought to have carved plateaus and valley networks, such as the ones
96 observed by the Huygens probe during its descent (Soderblom et al., 2007). Pure methane
97 cannot be solid at the surface because the surface temperature is quite homogeneous and
98 slightly above the freezing point of methane (Jennings et al., 2009). However, methane could
99 be trapped as methane clathrates. Methane is thus thought to play a central role in the moon's
100 atmospheric activity and meteorological cycle. Methane can form clouds, possibly rain down,

101 and collect on the surface and in sub-surface reservoirs that may then evaporate back to the
102 atmosphere (Flasar 1998; Tokano et al., 2001; Tokano, 2005; Atreya et al., 2006; Rannou et
103 al., 2006; Mitchell et al., 2006, 2009). Ethane is methane's major organic photochemical
104 byproduct (Yung et al., 1984; Toubanc et al., 1995). Liquid ethane has been identified in
105 Ontario Lacus probably in solution with liquid methane and other lower-molecular-mass
106 hydrocarbons and nitriles (Brown et al., 2008). Slightly less volatile than methane, ethane is
107 therefore thought to participate to a lesser extent in the liquids/solids cycle on Titan and also
108 to be the major constituent of the winter high latitude lakes and clouds (Griffith et al., 2006;
109 Rannou et al., 2006; Le Mouélic et al., in press). Both methane and ethane have the potential
110 to form clouds. The monitoring of Titan's clouds significantly contributes to the global
111 understanding of Titan's climate, meteorological cycles, and hydrocarbon cycles.

112 The first detections of transient cloud activity in Titan's atmosphere were achieved thanks
113 to spectroscopy and multispectral imaging from ground-based telescopes. The atmosphere of
114 Titan is opaque at visible and infrared wavelengths, except for some narrow spectral windows
115 where methane absorption is the weakest (for example in the near-infrared range at $\lambda = 0.93$,
116 1.08, 1.27, 1.59, 2.03, 2.75 and 5 μm – Titan's so-called atmospheric infrared windows).
117 Griffith et al. (1998) observed a significant brightening of Titan in the wings of the
118 atmospheric windows during September 1995, which was interpreted as a ~9% cloud cover of
119 the moon's disk. Griffith et al. (2000) also detected spectroscopic evidence for smaller scale
120 transient clouds occurring in several nights in 1993-1999 and covering less than 1% of Titan's
121 disk. Year 2002 marked the first report of Titan's clouds' direct imaging and localization
122 (Brown et al., 2002). Images were regularly obtained between 1996 and 2006 using Gemini
123 and Keck adaptive optics facilities (Brown et al., 2002; Roe et al., 2002; Gibbard et al., 2004;
124 de Pater et al., 2006; Schaller et al., 2006a, 2006b), the Canada France Hawaii Telescope and
125 Very Large Telescope along with adaptive optics systems (Hirtzig et al., 2006, 2007) and the

126 Palomar Hale telescope using the JPL adaptive optics system (Bouchez et al., 2005). These
127 large clouds, observed at Titan's south pole during maximum solar illumination, were at that
128 time thought to be predominantly composed of liquid or solid methane, demonstrating for the
129 first time the possibility of condensation and the large influence of localized seasonal moist
130 convection in Titan's atmosphere. These investigations from ground-based observations
131 gathered statistical constraints on Titan's cloud distribution in time and location - in particular
132 on the variability and periodicity of outburst and dissipation of the large south polar clouds
133 (Schaller et al., 2006a, 2006b).

134 Roe et al. (2005a, 2005b) reported the first detection between December 2003 and February
135 2005 of temperate-latitude cloud systems occurring at $\sim 40^\circ$ S. The preferential appearance of
136 clouds at the pole and mid-latitudes in the summer (southern at that time) hemisphere is
137 consistent with the predictions of Global Circulation Models (GCM) and can be explained by
138 the general circulation in Titan's atmosphere (Tokano et al., 2001; Tokano, 2005; Rannou et
139 al., 2006; Mitchell et al., 2006, 2009). The 40° S cloud band is triggered by the ascending
140 branch of the Hadley cell, while the south polar clouds result from the transport of methane
141 from warm mid-latitudes to cold polar latitudes. Roe et al. (2005b) also reported a striking
142 longitudinal clustering of mid-latitude clouds at that time and suggested a possible surface
143 control of the cloud activity of this region, such as local geysering or cryovolcanism. Finally,
144 Schaller et al. (2009) recently reported the Earth-based detection of a huge tropical storm.

145 Since July 2004, the Cassini mission has monitored Titan's clouds in unprecedented detail
146 on a monthly basis, which is very complementary to Earth-based observations. Two optical
147 cameras onboard Cassini have been used to image the clouds in Titan's atmosphere: 1) The
148 Imaging Science Subsystem (ISS) is a multi-spectral camera that can observe Titan's surface
149 and atmosphere thanks to several filters from the UV to the near-infrared (Porco et al., 2004),
150 2) The Visual and Infrared Mapping Spectrometer (VIMS) is an imaging spectrometer that

151 acquires hyperspectral images in 352 contiguous spectral channels between 0.3 and 5.2 μm
152 (Brown et al., 2004). Several clouds were already observed at both poles and summer mid-
153 and low-latitudes with ISS and VIMS during the first close flybys (Porco et al., 2005; Baines
154 et al., 2005; Griffith et al., 2005, 2006, 2009). Besides these isolated observations, statistics
155 on the location and time of appearance of ~ 50 clouds observed with ISS between 2004 and
156 2008 are given in Turtle et al. (2009). Turtle et al. (2009) also reported detection of clouds at
157 the tropics. The spectral dimension of the VIMS images allows the direct spectral detection of
158 cloud signatures and gives in addition access to the altitude of the clouds and the scattering
159 properties of their particles (Griffith et al., 2005, 2006, 2009; Rodriguez et al., 2009; Le
160 Mouélic et al., in press).

161 An accurate comparison of cloud coverage with GCM predictions requires the best available
162 temporal and spatial statistics. The models, however, have hitherto been poorly constrained
163 and their long-term meteorological predictions have not yet been observationally fully
164 verified. These models (e.g. Rannou et al., 2006; Mitchell et al., 2006, 2009) differ
165 significantly in their forecast by considering how Titan's atmospheric humidity, and therefore
166 the cloud coverage, shifts from one hemisphere to the other with the seasons. Constraining the
167 long-term evolution of Titan's meteorology is important to understanding if sustained cloud
168 coverage, rain, or storms could happen in tropical regions. It can help to appreciate if rainfalls
169 can occur near the Huygens probe landing site in the present day to create the observed
170 drainage channels - at the same latitudes where most of the land area is covered by
171 presumably dry equatorial dune fields. It can also provide constrains on whether a north-
172 south asymmetry in precipitation is present, which might then explain the asymmetry in
173 Titan's lake distribution (Aharonson et al., 2009).

174 The previously published long-term cloud survey from VIMS runs from July 2004 to
175 December 2007 (Rodriguez et al., 2009). More than 140 cloud events were found revealing

176 the evolution with time of their spatial coverage during almost half a Titan season during
177 southern summer. Although the spatial cloud coverage was in general agreement with the
178 GCM from Rannou et al. (2006), the non-detection of isolated clouds at latitudes of $\sim 40^\circ\text{N}$
179 and the persistence of the southern clouds at the end of 2007 while southern summer is ending
180 were in disagreement with the GCM (Rodriguez et al., 2009). The present paper extends the
181 study up to 2010 and provides additional constraints for the GCMs.

182 After describing the semi-automated methodology that we use to detect the clouds, this
183 paper provides time-averaged cloud coverage maps of Titan as well as latitude occurrence of
184 clouds versus time. This study expands in time the previous reports by Rodriguez et al. (2009)
185 and Brown et al. (2010) up to April 2010. It therefore provides a survey covering almost one
186 Titan season from early northern winter to the beginning of northern spring. Evolution during
187 that season and implications for GCMs and the comprehension of Titan's climatology are
188 discussed.

189

190 **2. Semi-automatic detection of Titan's clouds within VIMS images**

191

192 The VIMS imaging spectrometer observes Titan at global scale at low to medium resolution
193 (400 to 25 km/pixel), and at high resolution over a few percents of the surface, up to 500
194 m/pixel in localized areas (e.g. Barnes et al., 2008; Le Corre et al., 2009). A complete
195 description of the VIMS observations of Titan during the entire Cassini nominal mission (July
196 2004 – July 2008) is available in Barnes et al. (2009). Clouds systems are clearly visible in
197 several VIMS images at diagnostic infrared wavelengths (Baines et al., 2005; Griffith et al.,
198 2005, 2006, 2009; Rodriguez et al., 2009; Barnes et al., 2007, 2009). Between July 2004
199 (flyby T0) and April 2010 (T67), VIMS acquired more than 20,000 hyperspectral images of
200 Titan. By eliminating redundant, night side, limb viewing, very low time exposure and also

201 very small images, we reduced the dataset down to ~2,000 spectro-images useful for the
202 purpose of cloud detection. This still represents several millions of spectra and thousands of
203 images to inspect, preventing the efficient use of a manual detection technique alone. We
204 therefore developed a semi-automated algorithm to detect clouds in VIMS images (Rodriguez
205 et al., 2009). The basics of this method were already described in Rodriguez et al. (2009), and
206 are briefly summarized here.

207 Because clouds are efficient reflectors in the near-infrared and substantially reduce the path-
208 length of solar photons in Titan's atmosphere, their spectra present a significant and
209 simultaneous relative brightening of all atmospheric windows, which is not the case for
210 surface or limb spectra. Owing to these specific spectral signatures, the clouds on Titan can
211 therefore be distinguished from other atmospheric or surface features (Rodriguez et al., 2009).
212 The cloud-related brightening of the atmospheric windows mainly depends on the cloud top
213 altitude and composition, and on the size and number density of the droplets; this spectral
214 signature was the subject of other specific studies (Griffith et al., 2005, 2006, 2009).

215 We systematically analyzed several VIMS images with and without cloud features in order
216 to derive a spectral criterion that would be specific to the cloud spectral signature only. Some
217 specific surface features (such as Tui and Hotei Regio; i.e. Barnes et al., 2005, 2006 – see
218 Figure 1 in Rodriguez et al., 2009) show a particularly bright 5 μm window with very strong
219 signal relative to all other windows. On the other hand, cloud spectra always show
220 simultaneous brightening of all windows, particularly at 2.75 and 5 μm (see an example in
221 Figure 1 from Rodriguez et al., 2009). Taking into account the great variability of the VIMS
222 dataset in terms of resolution, illumination, emission and phase angles, we empirically found
223 that the most robust detection criterion to separate pixels that contain a “cloudy” spectral
224 component from any other component is to use the simultaneous brightening of the 2.75 and 5

225 μm windows. We found that taking a single window or a combination of two other windows
226 leads repeatedly to false positive detections.

227 We then developed an algorithm that automatically calculates the 2.75 and 5 μm window
228 areas for every pixel of each VIMS datacube. These areas are defined as the integrals of the
229 reflectance between 2.35 and 3.21 μm for the 2.75 μm window and between 4.74 μm and 5.11
230 μm for the 5 μm window. For each VIMS cube, a 2D scatter plot of areas at 5 μm versus
231 areas at 2.75 μm is then built. In this new space of representation, most of the pixels of the
232 cube are statistically distributed within a Gaussian shape, except for pixels with a cloud
233 contribution that are clustered in the “high-value” wing of the distributions (see 2D scatter
234 plot in Figure 1, Rodriguez et al., 2009). Two-sigma conservative thresholds on the two area
235 distributions are automatically calculated in order to select only pixels corresponding to
236 clouds. Each selection is then visually checked and the thresholds are eventually tuned to
237 assure that all detections are real and that we do miss as few “cloudy” pixels as possible. We
238 still deliberately choose conservative thresholds to avoid false positives. This can lead to the
239 non-detection of optically thin or very low clouds, of clouds that are much smaller than a
240 VIMS pixel, or of clouds that are too close to the limb (see **Table A1** from the **Appendix**).

241 Finally, once the “cloudy” pixels are selected by our algorithm within an image, they are
242 reprojected on Titan’s globe. This process is repeated for each of the 2,000 selected VIMS
243 datacubes spanning 2004 to 2010, to produce the final detection maps and time evolution
244 plots. The reprojection of VIMS pixels on Titan’s globe is the essential final step of our
245 computations and is carried out by navigating the Cassini observations. The navigation is the
246 mathematical process that assigns longitude and latitude coordinates to the four corners of
247 each pixel on the image plane, as well as geometric information such as incidence, emergence
248 and phase angles. We developed software that (1) calculates the rotation matrix of the VIMS
249 focal-plane-based coordinate system to the planet-based coordinate system, (2) applies this

250 rotation to all the image pixels, and (3) computes the intersection with the planet ellipsoid
251 expressing the results in terms of longitude and latitude coordinates. Our navigation code uses
252 functions of the ICY toolkit and ancillary data stored in SPICE kernels (Spacecraft Planet
253 Instrument C-matrix Event) provided by the NAIF (Navigation and Ancillary Information
254 Facility; <http://naif.jpl.nasa.gov/naif/>). This code was already successfully
255 applied to VIMS images of Titan, for surface studies and cartography (Sotin et al., 2005;
256 Rodriguez et al., 2006; Le Mouélic et al., 2008b; Le Corre, et al., 2009), as well as for haze
257 study and cloud tracking (Le Mouélic et al., 2008a; Rodriguez et al., 2009; Rannou et al.,
258 2010).

259 This cloud mapping algorithm has been recently improved by introducing capabilities to (1)
260 select regions of interest, (2) mask Titan's bright limb that often prevented the detection of the
261 dimmest clouds, and (3) help the visual checking of the detections using the 2.1 μm VIMS
262 channel, which is sensitive to tropospheric clouds. All the cloud detection maps shown in this
263 study were produced with this new version of the detection algorithm.

264 Brown et al. (2010) pursued an alternate approach by using pure visual cloud detection. See
265 the **Appendix** for a detailed comparison of the two methods and their results.

266

267 **3. Results**

268

269 **3.1 Global view of the 2004-2010 cloud coverage of Titan**

270

271 Using the method described in **Section 2**, we select only cloud pixels within the whole
272 VIMS dataset between July 2004 (Cassini flyby tagged T0) and April 2010 (T67). The
273 selected pixels are gathered in time clusters corresponding to the duration of each individual
274 Titan targeted-flyby and are then reprojected into the planetocentric Titan coordinate system

275 to produce the 67 individual cloud detection maps shown in **Figure 1**. These maps use as
276 background a VIMS global mosaic with a mask corresponding to the dayside coverage
277 recorded during the corresponding flybys. From T0 up to T38, the maps presented here
278 correspond to updated versions of the one presented in Rodriguez et al. (2009). They
279 comprise 20 new detections and include shape improvements for six previous detections (see
280 the **Appendix** for details). The total of 220 clouds shown in our detection maps are all
281 referenced and documented in **Table A1** of the **Appendix** to allow further comparisons with
282 other studies.

283

284 **[Figure 1]**

285

286 **Figure 2a** summarizes both the data analyzed and the clouds detected during the six-year
287 period. The cumulative number of cloud observations between July 2004 and April 2010 is
288 illustrated in **Figure 2b**. It corresponds to the number of times that a cloud has been observed
289 by the VIMS instrument at a given location. The cloud count varies from 0 to 30, with a mean
290 value of 2. The total number of VIMS observations at a given point is mapped in **Figure 2c**.
291 This number varies between 1 and 53, with a mean number of 29. The fractional cloud
292 coverage (**Figure 2d**) is calculated by dividing the number of cloud occurrences at a given
293 latitude/longitude location (**Figure 2b**) by the number of VIMS observations of that location
294 (**Figure 2c**). This operation compensates for the systematic biases coming from the widely
295 varying VIMS coverage. It is important to consider all of these maps together when drawing
296 conclusions. For example, there seem to be less cloudy areas well localized in the northern
297 polar region at $\sim 90^\circ\text{E}$ and -45°E longitudes (holes in the uniform north polar cloud blanket).
298 These particular areas correlate, in fact, with a lower sampling. Indeed these particular regions
299 were imaged only 0 to 10 times by VIMS, with very coarse spatial resolution (greater than

300 200 km per pixel) and often in limb viewing conditions; hence their identification as ‘holes’ is
301 statistically insignificant. Elsewhere on Titan, the VIMS coverage is sufficient to consider the
302 averaged fractional cloud coverage presented in **Figure 2d** with higher confidence.

303

304 **[Figure 2]**

305

306 On a global scale, Titan’s cloud coverage is very low relative to terrestrial standards, with a
307 very patchy cloud coverage. Averaged over the period interval between July 2004 and April
308 2010, the cloud coverage only represents ~10% of Titan’s entire globe. In comparison, the
309 instantaneous cloud coverage on Earth is seven times greater (~75%) on average (Mace et al.,
310 2009). Between northern winter and the beginning of spring (the 2004-2010 period), Titan’s
311 clouds have mostly occurred in three areas which are well delineated in latitude (**Figure 2d**):
312 1) the north polar region, 2) the temperate southern latitudes, and 3) the south pole. Other
313 regions are almost completely free of clouds, except for very sporadic tropical outbursts and
314 two small clouds at northern mid-latitudes (~40°N).

315

316 **3.2 Time evolution of Titan’s cloud activity from 2004 (winter) up to 2010 (spring)**

317

318 The seasonal evolution of the large-scale geographic distribution of clouds is a strong
319 marker of the global atmospheric circulation on Titan (Tokano et al., 2001; Tokano, 2005;
320 Rannou et al., 2006; Mitchell, 2006, 2009; Turtle et al., 2009; Rodriguez et al. 2009). We
321 present in this section the time evolution of the main cloud structures that we identified in our
322 observations. **Figure 3** shows the time evolution of the latitudinal distribution of Titan’s
323 clouds between July 2004 (winter) and April 2010 (spring) as seen complementarily by Earth-
324 based telescopes (Roe et al., 2005b; Schaller et al., 2006b; de Pater et al., 2006; Hirtzig et al.,

325 2006; Schaller et al., 2009) and Cassini (Porco et al., 2005; Baines et al., 2005; Griffith et al.,
326 2005, 2006; Le Mouélic et al., 2008a; Turtle et al., 2009; Rodriguez et al., 2009; and this
327 study). **Figure 4** also presents the evolution of Titan's cloud cover during the same period, but
328 provides additional information on the regional evolution of this distribution by showing
329 maps of fractional cloud coverage over four time periods. This figure shows the global and
330 latitudinal fractional cloud coverage for four periods from Cassini flyby T0 (1st of July 2004)
331 up to T16 (22 July 2006), T17 (7 September 2006) up to T40 (5 January 2008), T41 (22
332 February 2008) up to T58 (8 July 2009), and T59 (24 July 2009) up to T67 (5 April 2010).

333

334 **[Figure 3]**

335 **[Figure 4]**

336

337 *3.2.1 North polar cloud*

338

339 The northern polar region of Titan is systematically blanketed by an ever-present thin cloud
340 system from the first Cassini observations in mid-2004 until early 2008. As Titan's north pole
341 progressively emerges from the night, this large, stratiform cloud system is found to cover the
342 polar region at all longitudes and from ~60°N latitude up to the pole (Griffith et al., 2006; Le
343 Mouélic et al., 2008a; Rodriguez et al., 2009; Le Mouélic et al., in press). Poleward of ~60°N
344 the fraction of cloud coverage, averaged over the 2004-2010 period, is greater than 70%
345 (**Figure 2d**). Its total surface coverage however has slightly diminished with time. Very stable
346 between 2004 and 2006, with an overall fractional coverage greater than 80% (black curve in
347 **Figure 4e**), this large cloud started slowly recessing since mid-2006 (blue curve in **Figure**
348 **4e**). After mid-2008, the north polar cloud began to fractionate and collapse at some places,
349 leaving a cloud ring centered at ~60°N with only small, but more opaque and convective-type

350 cloud patches in its central region (**Figures 1, 3, 4c** and green curve in **Figure 4e**). Later on,
351 as Titan passed the spring equinox in August 2009, all that had remained from the large north
352 cloud cap, including the thin $\sim 60^\circ\text{N}$ cloud ring, finally disappeared, leaving the north pole
353 free of cloud, apart from small and sporadic clouds (**Figures 1, 3, 4d** and red curve in **Figure**
354 **4e**), likely to be convective in nature. A detailed analysis of the Titan's north polar cloud
355 seasonal recessing can be found in Le Mouélic et al. (in press).

356

357 *3.2.2 South polar outbursts*

358

359 Large clouds are also clearly visible at the south pole since the early VIMS observations of
360 Titan in 2004 (**Figures 1, 3 and 4a**). Cloud events at Titan's south pole have been previously
361 reported from Earth-based observation campaigns since December 2001 (Brown et al., 2002;
362 Roe et al., 2002; de Pater et al., 2006; Hirtzig et al., 2006; Schaller et al., 2006a, 2006b,
363 2009). From telescopic observations, these clouds appeared to be tropospheric large scale
364 stormy outbursts with variability timescales (related to their changes in size and/or height) of
365 a few hours (Schaller et al., 2006a). These storms have sustained their activity almost
366 continuously until November 2004, from which time they were also observed by Cassini
367 (Porco et al., 2005; Baines et al., 2005; Turtle et al., 2009; Rodriguez et al., 2009; this study).
368 Contrary to what was previously thought from Earth-based imaging (Schaller et al., 2006b),
369 south polar clouds have still retained a substantial activity after this date. They were indeed
370 constantly detected by VIMS after November 2004 up to December 2005, during almost all
371 Cassini flybys of Titan (**Figures 1 and 3**). Nevertheless these events were dimmer and less
372 spatially extended than those seen since 2002, possibly preventing Earth-based telescopes
373 from resolving them. After December 2005, the cloud activity at the south pole began to
374 decline. For the first time since 2001, no clouds near the south pole were observed for 8

375 months, between January and September 2006 (**Figures 1 and 3**). Large outbursts were then
376 regularly detected again for almost a year (**Figures 1, 3, 4b and 4c**). Except for some rare and
377 small scale events in 2008, the south pole of Titan ceased all stormy activity starting from the
378 last dissipation in mid-2007, two years before the northern spring equinox (**Figures 1, 3, 4c**
379 **and 4d**). This decline is illustrated by the gradual decrease of the mean fractional coverage in
380 clouds poleward of 60°S between 2004-2006 (~15%) and 2009-2010 (down to 0%) periods
381 (black to red curve in **Figure 4e**).

382

383 *3.2.3 Southern mid-latitude clouds*

384

385 On the other hand, southern mid-latitude clouds were observed by ISS (Turtle et al., 2009)
386 and VIMS (Rodriguez et al., 2009; this study) on a regular basis between July 2004 and April
387 2010 (**Figures 1 and 3**). Indeed, recent VIMS observations show that southern mid-latitudes
388 (regions of Titan between 30°S and 60°S) showed a relatively stable fractional coverage in
389 clouds of ~10% during the entire 2004-2010 time interval (**Figures 4a to 4e**), reaching a peak
390 mean fractional coverage of ~15% between July 2009 and April 2010. These clouds were thus
391 still present, and quite active, at the time of the northern spring equinox (August 2009), and
392 do not seem to display any sign of decline after that date thus far. Southern mid-latitude
393 clouds are generally found to be elongated in the east-west direction, likely stretched by zonal
394 wind shear at the altitude where they form (Griffith et al., 2005; Rodriguez et al., 2009).

395

396 *3.2.4 Tropical and northern mid-latitude clouds*

397

398 After December 2006, we identify some clouds further north in Titan's tropics, equatorward
399 of $\pm 30^\circ$ latitudes (green to reddish colors in **Figures 1 and 2a**). Most of them are found in the

400 southern hemisphere (**Figures 1, 2a and 3**). Some of these clouds were also reported in other
401 studies (Porco et al., 2005; Griffith et al., 2009; Turtle et al., 2009; Rodriguez et al., 2009;
402 Schaller et al., 2009). However, contrary to what we observed in the high- to mid-latitude
403 regions of the southern hemisphere, these near-equatorial clouds were in general much
404 smaller (except for the T56 and T65 events) and significantly more scarce, appearing in less
405 than ~5% of the 67 Cassini flybys between July 2004 and April 2010 (**Figures 2d and 4**).
406 Their scarcity is not due to a spatial resolution effect. Indeed, for example, the small tropical
407 clouds observed during the T41 flyby (22 February 2008) were detected with a mean spatial
408 resolution of 70 km/pixel, demonstrating the capability of VIMS to detect clouds with such a
409 coarse resolution, with which more than 90% of Titan's surface has been imaged. Despite
410 their scarcity, we notice that equatorial clouds appear with a slightly higher frequency after
411 February 2008, during the approach of equinox.

412 Finally, we also observe the first, consecutive appearances of two small elongated clouds at
413 northern mid-latitudes (flybys T62 and T63 in **Figure 1, Figure 4e and 7**). These unique
414 clouds have an elongated morphology similar to the ~40°S clouds, and are not connected to
415 the north polar cloud (orange color in **Figures 1 and 2a**). They first appeared in late 2009,
416 right after the northern spring equinox (**Figure 3** and red curve in **Figure 4e**), and were
417 observed while ~40°S clouds were still active.

418

419 **4. Discussion**

420

421 **4.1 General circulation and Titan's climate: comparison with predictions of GCMs**

422

423 The observation of Titan's cloud distribution and its evolution with season provides critical
424 constraints on models of Titan's atmospheric circulation. Comparing the common features

425 and the differences between observations and predictions can drive enhanced comprehension
426 of the physical processes controlling Titan's general circulation. Among the GCMs available
427 for Titan that incorporate moist processes (Tokano et al., 2001; Tokano, 2005; Rannou et al.,
428 2006; Mitchell et al., 2006, 2009; Newman et al., 2008), we compare here two models that
429 document in detail the seasonal evolution of clouds and/or precipitation (Rannou et al., 2006;
430 Mitchell et al., 2006, 2009). Both are two-dimensional axisymmetric (altitude-latitude). Yet,
431 the physical processes that drive the dynamics of Titan's atmosphere and the cloud formation
432 differ markedly from one model to the other. The Mitchell et al. (2006, 2009) model 1) is
433 tropospheric only, 2) does not include the haze, 3) omits horizontal mixing processes, and 4)
434 enables methane condensation where and when its atmospheric saturation ratio exceeds unity
435 through parameterized moist convection. The methane condensation 'instantly' triggers
436 precipitation, unless underlying atmosphere is subsaturated. The IPSL-TGCM (for Institut
437 Pierre-Simon Laplace - Titan's General Circulation Model; Rannou et al., 2006) 1) goes up to
438 the mesosphere at ~500 km altitude and dynamically couples all the atmospheric layers, 2)
439 accounts for horizontal diffusion (by eddy angular momentum transport due to barotropic
440 instabilities), 3) does not include moist convection, but 4) calculates and couples the haze and
441 cloud microphysics regarding nucleation, methane and ethane condensation, and
442 sedimentation (see Lebonnois et al. (2009) for a detailed review of the IPSL-TGCM). The
443 different physics used by the two models lead to radically distinct predictions for the
444 tropospheric cloud/precipitation seasonality. An abrupt shift of the meteorology from the
445 winter to the summer hemisphere, only interrupted by a quiescent period of 3-4 terrestrial
446 years after the equinox, is forecast by the IPSL-TGCM. On the contrary, the Mitchell et al.
447 (2009) model predicts a smooth, continuous migration of precipitation from one hemisphere
448 to the other between solstices. The time evolutions of Titan's cloud/precipitation latitudinal

449 coverage as predicted by the Mitchell et al. (2009) model and the IPSL-TGCM (Rannou et al.,
450 2006) are compared in **Figure 5**.

451

452 **[Figure 5]**

453

454 *4.1.1 Cloud preferential latitudes during Titan's winter*

455

456 In the summer hemisphere, both model predictions for the preferential latitudes of
457 cloud/condensation are very similar and in satisfactory agreement with the latitudinal
458 distribution of the main tropospheric cloud structures that are observed: the mid-latitude band
459 and the polar outbursts. Both models predict methane clouds or condensation to form at mid-
460 latitudes in the summer hemisphere ($\sim 40\text{-}60^\circ$), precisely as observed by ISS (Turtle et al.,
461 2009) and VIMS (Rodriguez et al., 2009; this study). This region corresponds in the GCMs to
462 the rising branch of the tropospheric Hadley cell (the equivalent of Earth's Intertropical
463 Convergence Zone, ITCZ). Both GCMs also predict sporadic methane clouds and
464 precipitation to occur in the summer polar region. The Mitchell et al. (2006, 2009) model
465 suggests that these polar clouds are caused by a complex of polar vertical moist convection of
466 methane-rich air cells (Hueso and Sanchez-Lavega, 2006; Barth and Rafkin, 2007) that occurs
467 only at summer pole. Alternatively, Rannou et al. (2006) propose that the convection and
468 condensation is triggered very close to the summer pole by the existence of a slantwise
469 circulation cell, forced by the temperature gradient, which brings methane-rich air from lower
470 latitudes to the higher and colder latitudes. The convective nature of the summer hemisphere
471 events, as predicted by the models, is consistent with the morphology and the transience of the
472 clouds observed in the southern hemisphere during summer (Brown et al., 2002; Porco et al.,
473 2005; Schaller et al., 2006a, 2006b). However, the match in latitudes between the GCMs

474 predictions for the summer hemisphere and the observations is less accurate in the polar
475 region than in the mid-latitudes. Neither of the two models produces significant cloud
476 cover/condensation at 65-85°S where most of the numerous convective polar clouds are
477 observed. Nevertheless, the gap in cloud activity between ~50° and 65°S is well predicted by
478 both GCMs.

479 The IPSL-TGCM predicts methane clouds at mid-latitudes in the winter hemisphere. Less
480 intense than in the summer hemisphere, cloud activity at northern mid-latitudes is
481 nevertheless expected by the IPSL-TGCM throughout most of southern summer. We do not
482 see any, though. Indeed, no clouds were detected before the equinox in the 0-50°N latitudes
483 by ISS (Turtle et al., 2009) or by VIMS (Rodriguez et al., 2009; this study). In comparison,
484 the Mitchell et al. (2006, 2009) model does not predict any methane condensation in the
485 winter hemisphere. As stated in Rodriguez et al. (2009), the erroneous prediction of the
486 ~40°N clouds by the IPSL-TGCM during the southern summer is a failure of the model. In
487 the IPSL-TGCM, the winter ~40°N clouds are not associated with the general circulation, the
488 rising branch of the tropospheric Hadley cell being locked at southern mid-latitudes. These
489 clouds in the model are rather associated with latitudinal transport of methane by eddy
490 diffusion, produced by inertial instabilities, through the equator-to-pole temperature gradient.
491 This differs from clouds produced by ascending motions, as for instance at ~40°S in the
492 summer hemisphere. Rodriguez et al. (2009) showed that the IPSL-TGCM overestimates the
493 equator-to-pole temperature contrast in the winter hemisphere by a least a factor two relative
494 to what was measured by the CIRS instrument onboard Cassini (Jennings et al., 2009). This
495 could explain why, in consequence, the model overestimates the efficiency of methane
496 condensation and cloud formation at ~40°N during southern summer.

497 On the other side, the IPSL-TGCM predicts the appearance and the observed latitude of the
498 widespread winter polar cloud with high fidelity. This polar cloud system is assumed to be

499 stable over the winter season resulting from the tropospheric cooling of descending
500 stratospheric air (Rannou et al., 2006). The descending winter polar branch of the
501 stratospheric circulation is expected to bring air cells enriched in ethane and aerosols down to
502 an altitude of ~30-60 km near the tropopause where the ethane can condense, above the
503 altitude of methane condensation, which is in very good agreement with the Cassini/VIMS
504 “from above” observations of Titan’s north polar region (Griffith et al., 2006; Le Mouélic et
505 al., in press). This pole-to-pole circulation supplies the winter polar vortex, poleward of
506 ~60°N, in large-scale drizzle of small ethane-rich particles which may settle and eventually
507 replenish ethane in the northern lakes. The underlying polar methane clouds, even if present
508 and more opaque, may be hidden from Cassini view by the extensive overlying ethane cloud
509 layer. Methane clouds at lower altitude would become more clearly visible only when the
510 ethane cloud starts to thin out, fractionate and disappear. It is worth noting that the non-
511 prediction of this cloud by Mitchell et al. (2006, 2009) is not a failure, since their model is
512 only tropospheric and does not incorporate the ethane cycle.

513

514 *4.1.2 The seasonal evolution of the cloud cover, from winter to spring*

515

516 With the most recent resolved observations through and beyond the northern spring equinox
517 reported in this study, we have the opportunity to make specific comparisons, not only about
518 the cloud distribution in latitude, but also about its time evolution.

519 The progressive disappearance of the north polar cloud, as monitored by VIMS between
520 2006 and 2010 (this study and Le Mouélic et al., in press), is predicted by the IPSL-TGCM
521 with the correct timing (Le Mouélic et al., in press). According to the model, the recession of
522 the winter polar cloud is a clear sign of the onset of the circulation turnover that affects the
523 descending branch of the stratospheric cell in the winter polar region.

524 In the opposite hemisphere, summer high- and mid-latitude cloud activity persists much
525 longer than predicted by the IPSL-TGCM during approach to Titan's equinox. As observed
526 by VIMS, the entire summer hemisphere experiences a significant time lag in the seasonal
527 evolution of the cloud cover. According to the model, the southern polar clouds should have
528 entirely disappeared since mid-2005, whereas we still observe significant cloud activity in
529 these regions until mid-2008. This time lag was already documented in Rodriguez et al.
530 (2009). Nonetheless, the complete disappearance of the southern polar cloud after 2009
531 provides more evidence for the onset of the tropospheric circulation turnover, even if delayed.
532 Our recent observations do not yet show the $\sim 40^\circ$ s cloud activity disappearing, as predicted
533 by the IPSL-TGCM to occur starting in mid-2007, though it is still possible that this will
534 occur following a larger time lag. Since clouds are directly linked to the general circulation,
535 these differences indicate that the Hadley cell persists longer in reality than in the IPSL-
536 TGCM. There are two possibilities. First the thermal inertia of the ground may be greater than
537 assumed in the model, as was first postulated by Rodriguez et al. (2009). However this is not
538 likely since the value that the IPSL-TGCM used ($2000 \text{ J.m}^{-2}.\text{s}^{-1/2}.\text{K}^{-1}$) is already larger than
539 the expected values for Titan ($\sim 500 \text{ J.m}^{-2}.\text{s}^{-1/2}.\text{K}^{-1}$, see Tokano, 2005). A second, more
540 satisfying explanation for the persistence of convective activity in the summer hemisphere
541 brings into play the strong interaction between the ground humidity and the atmosphere.
542 Mitchell et al. (2009), which reproduced more faithfully the observed persistence of $\sim 40^\circ\text{S}$
543 clouds, also showed that they can produce a time lag in the seasonal occurrence of clouds up
544 to 3-4 terrestrial years by adjusting the importance of methane latent heat effects (done by
545 varying the surface boundary layer humidity). In comparison, in Rannou et al. (2006), the
546 methane source is set with a simple evaporation law from an infinite surface reservoir. Other
547 prescriptions of the methane source, with different geographical distribution of liquid

548 methane, and a complete feedback with the precipitation rate and location, will be tested in
549 the future with the IPSL-TGCM.

550 Not seen during the whole northern winter, clouds are detected for the first time with VIMS
551 at $\sim 40^\circ\text{N}$ latitude on two occasions during the T62 (12 October 2009) and T63 flybys (12
552 December 2009), a few terrestrial months after equinox (**Figure 1** and details in **Figure 6**).
553 According to the GCMs (Rannou et al., 2006; Mitchell et al., 2006, 2009), the perennial
554 appearance of these northern mid-latitude clouds should be the markers of the completion of
555 the seasonal atmospheric circulation turnover at the end of Titan's spring (which should not
556 occur before 2015-2017 - see **Figure 5**). Although single events are always hazardous to
557 interpret, we can nevertheless point out that such early springtime clouds are unlikely to be
558 associated with an early hemispherical shift of the ITCZ to the north (which is predicted to
559 occur during the equinoctial transition phase and to take 3-4 terrestrial years after the equinox
560 to complete (Rannou et al., 2006; Mitchell et al., 2009)). As the Hadley cell present in a
561 planetary atmosphere is directly produced by and strongly linked to the seasonal solar forcing,
562 only one ascending branch is expected to occur at a given time. If these $\sim 40^\circ\text{N}$ clouds were
563 related to a rising branch of the tropospheric Hadley cell, and therefore with the completion of
564 the circulation turnover within the troposphere, we would not have observed the systematic
565 coexistence of such events with persistent clouds at $\sim 40^\circ\text{S}$ (this latter being likely to be
566 associated with the ITCZ still locked in the southern hemisphere at the end of southern
567 summer and the very beginning of northern spring). It is thus impossible for the circulation
568 turnover process to be at the same time delayed in the southern hemisphere and in advance in
569 the northern hemisphere. However, the onset of the circulation turnover and the motion of
570 solar insolation towards the north may modify the condition of latitudinal transport from the
571 tropics towards the north pole (strengthening of the eddy diffusion) and may occasionally
572 produce more clouds further north, where no large scale upward motions are expected. GCMs

573 generally predict large scale circulation and may miss local, but strong circulation able to
574 produce ascending motion and clouds. If we consider that the ITCZ stays locked at summer
575 mid-latitudes (Rannou et al., 2006), as suggested by the invariable observation of clouds at
576 $\sim 40^{\circ}\text{S}$, local scale circulations could explain the more frequent occurrence of clouds near the
577 equator, as Titan is going through and beyond equinox and tropics are more and more
578 powered by solar illumination. Another explanation is that such singular events may also be
579 related to events totally external to climatology, such as strong degassing from the ground.
580 Only the long-term monitoring of these latitudes will help to discriminate between these
581 possibilities.

582

583 **[Figure 6]**

584

585 The combination of 1) the cessation of ‘winter-type’ cloud activity at both poles (convective
586 clouds at the south pole and large ethane cloud cap at the north pole), 2) the constant
587 appearance of clouds at 40°S through mid-2010, 3) the occurrence, a few months before and
588 after the equinox, of more frequent equatorial clouds, and 4) the first appearance of northern
589 mid-latitude clouds clearly indicates the onset of the circulation turnover and seems to imply
590 an ‘abrupt’ hemispherical reversal of cloud activity, as predicted by the IPSL-TGCM, rather
591 than a gradual migration of precipitation from the southern to the northern hemisphere
592 (Mitchell et al., 2006, 2009). Nevertheless, as our monitoring in the present work ceases in
593 April 2010, we still lack cloud observations after the equinox and the observation of Titan’s
594 meteorology during the entire equinoctial transition phase will be essential to understanding
595 the real nature and timescale of the circulation turnover.

596

597 **4.2 Longitudinal distributions of clouds**

598

599 The only GCMs that predict and map the evolution of the cloud cover (Rannou et al., 2006)
600 or methane precipitation (Mitchell et al., 2006, 2009) are only a 2D representation, in latitude
601 and altitude. Therefore, they do not predict longitudinal variations in the cloud coverage. At
602 the north pole, where ethane clouds are predominantly formed by downwelling, no
603 longitudinal variations are expected. On the other hand, the clouds in the summer hemisphere
604 are formed by upwelling which can be affected by surface properties such as topography,
605 hydrocarbon sources (lakes, cryovolcanism) and temperature, and by wave propagation in the
606 lower atmosphere. The observation of the distribution of clouds with longitude allows further
607 exploration of the possible interaction between the general atmospheric circulation and
608 processes that are related to the surface or to external forcing (e.g., Saturn's tides).

609

610 *4.2.1 The south pole area during southern summer*

611

612 **Figure 7** shows the fractional cloud coverage for the southern high latitudes for two
613 successive periods: 2004-2007 and 2007-2010. **Figure 7d** shows in particular the fractional
614 cloud coverage as a function of longitudes averaged between 90°S and 60°S, for these two
615 periods. Between 2004 and 2007, in the middle of southern summer, the south pole fractional
616 cloud coverage presents significant variations with longitude (**Figure 7b** and blue curve in
617 **Figure 7d**). At these latitudes and during that period, the cloud coverage was globally greater
618 in the leading hemisphere (between -180°E and 0°) than in the trailing. This distribution
619 clearly peaks at ~10% of fractional coverage at -120°E, 60°E eastward of Ontario Lacus
620 (**Figure 7a**), the largest lake of the southern high latitudes, with some spreading around the
621 anti-Saturn point (180°E), just above the lake. The 2007-2010 period shows an obvious
622 decline in cloud activity in the southern polar region, as summer ends and fall begins (**Figure**

623 **7c** and red curve in **Figure 7d**). Nevertheless, at that time as well, notable cloud coverage
624 occurs only near Ontario Lacus and eastward of it. In contrast, the opposite side of Titan,
625 around 90°E, shows few to no clouds throughout the observation period.

626

627 **[Figure 7]**

628

629 The curves of the fractional cloud coverage as function of longitude for the 2004-2007 and
630 2007-2010 periods have a very similar shape (**Figure 7d**). At first order (large scale), it seems
631 that one can go from one to the other by only applying a multiplicative factor. This implies
632 that the processes governing the localization of south pole clouds in the leading hemisphere
633 between 2004 and 2007 and between 2007 and 2010 must have a similar origin. A possible
634 explanation is that Ontario Lacus, helped by the polar pattern of the general circulation (very
635 active in the middle of the southern summer) and of the zonal winds, may act as a local
636 catalyst for cloud formation and clustering (Brown et al., 2009; see **Figure 8**). Ontario Lacus
637 is the largest, and only stable lake filled with liquid hydrocarbons yet identified in Titan's
638 south polar regions (Brown et al., 2008; Turtle et al., 2009). As methane, and ethane to a
639 greater extent, has a very low evaporation rate under Titan's surface conditions (Mitri et al.,
640 2007), Ontario Lacus is expected to evaporate only by a few meters and to be large and deep
641 enough to persist over seasons, at least during the last few thousands of years (Aharonson et
642 al., 2009; Wall et al., 2010; Hayes et al., 2010). During summer in the southern hemisphere,
643 the local surface and near surface humidity would increase in the vicinity of this natural
644 reservoir of liquid hydrocarbons with an efficiency higher than anywhere else in the south
645 polar regions. At the same time, a small and oblique tropospheric circulation cell is expected
646 to occur in the south polar regions (Rannou et al., 2006), with an ascending branch rising up
647 to altitudes of 20 to 30 km above the pole. The interplay between the large-scale polar

648 circulation cell and the presence of Ontario Lacus would bring upward the local excess of
649 humidity to altitudes where it can condense and form clouds (see Tokano (2009) for a detailed
650 study of the impact of lakes on winter/summer polar meteorology on Titan). Zonal winds at
651 that epoch (southern summer) and these latitudes (between 90°S and 60°S) are predicted by
652 GCMs to be almost null to slightly retrograde (westward) at very low altitude and globally
653 prograde (eastward) above 10 km with a wind speed of ~1 m/s (Tokano and Neubauer, 2005;
654 Rannou et al., 2006). That prediction is consistent with prograde wind speeds of a few meters
655 per second retrieved at these latitudes from cloud tracking (Porco et al., 2005). These
656 eastward winds would continuously push to the east these methane-rich rising air parcels,
657 resulting in clouds preferentially formed eastward of Ontario Lacus. This effect is limited by
658 the time scale of polar methane clouds sedimentation and lifetime, which is of the order of a
659 few hours to a few days (Rannou et al., 2006). These clouds could be therefore transported
660 eastward by this mechanism from 50 km up to 300 km before rainout occurs, which
661 corresponds at these latitudes to 30°-180° of possible longitudinal excursion east of Ontario.
662 This scenario, also supported by the calculations of Tokano (2009), is fully consistent with the
663 distribution of clouds observed by VIMS (**Figure 7b**). The predicted zonal winds are only an
664 average value and it is possible that some clouds could also, but more rarely, stay stationary
665 above Ontario or reach regions slightly westward of it, as is also observed by VIMS (**Figure**
666 **7b**). ISS images of the south polar regions showed that convective clouds and changes in
667 surface brightness occurred between 2004 and 2005 (Turtle et al., 2009) at the place where
668 VIMS observed the maximum of the south pole cloud distribution (see **Figure 7a and 6b**).
669 Indeed at ~-120°E longitude and in the 70°-80°S latitude range, ISS reported recent
670 darkenings of the surface attributed to sporadic apparitions of liquid-filled depressions or
671 ponds due to local and seasonal meteorology, in very good agreement with our scenario. The
672 intensity of these processes must therefore be modulated by the general decline of southern

673 cloud activity during seasonal change, when solar insolation energy flux diminishes, as it is
674 indeed observed by VIMS (**Figure 7c**).

675

676 **[Figure 8]**

677

678 *4.2.2 Tidal control*

679

680 We conducted a similar study of the cloud coverage distribution with longitudes for the
681 mid-latitudes of Titan. **Figure 9** shows the fractional cloud coverage for the southern mid-
682 latitudes for the same two successive periods of **Figure 7**: 2004-2007 (dead of southern
683 summer) and 2007-2010 (end of southern summer and beginning of southern fall). The
684 fractional cloud coverage as a function of longitude, averaged between 35° and 55°S, is
685 presented in **Figure 9d**, for these two periods and an additional previous period of
686 observations (2003-2005) obtained by an Earth-based campaign (Roe et al., 2005b). There is
687 only a six-month overlap between the Roe et al. (2005b) study and our first group of
688 observations. As stated in Roe et al. (2005b) and Rodriguez et al. (2009), we observe
689 significant longitudinal structures within the mid-latitude cloud distribution throughout the
690 period between 2003 and 2010. After equinox, Titan's meteorology remained active at mid-
691 latitudes (see **Section 3.2**). The distribution of cloud coverage with longitude shows a
692 prominent peak of cloud activity roughly centered on the region facing Saturn ($0^{\circ}_{-10^{\circ}}^{+30^{\circ}}$ of east
693 longitudes). This region never dropped below 18% in cloud fractional coverage, reaching
694 25% during the 2007-2010 period. A secondary peak about a third lower in intensity seems to
695 emerge near the opposite side of Titan at ~180°E (near the centre of the anti-Saturn
696 hemisphere). Elsewhere, the fractional coverage never exceeded 10% on average during this
697 time interval. We have now sufficient statistics in time coverage and number of cloud

698 detections to consider that both of the peaks we observe with VIMS are real. However, it is
699 possible that the displacement of the main peak of about 30° eastward between 2003-2005
700 and 2004-2007 reported by Rodriguez et al. (2009) was only due to statistical effects, as we
701 observe now that three years later it returned, with no satisfactory explanation, to its early
702 position reported in 2003-2005 by Roe et al. (2005b). The fact remains that the n=2-mode
703 wave pattern of the mid-latitude longitudinal cloud distribution, still present in 2010, as well
704 as the loose correlation of the peaks of this distribution with any remarkable surface features,
705 plead for an atmospheric origin for the cloud structuring in longitude. As proposed by
706 Rodriguez et al. (2009), the sub- and, at a lesser extent, anti-Saturn bumps strongly suggest an
707 external forcing by Saturn's tides. This mechanism, already suspected to generate strong and
708 sudden changes in zonal winds patterns at some preferential longitudes 180° apart, due to
709 interaction with perturbed vertical winds (Tokano and Neubauer, 2002), could also act to
710 enhance or inhibit cloud formation in these locations. This hypothesis still needs to be tested
711 by GCMs for Titan which include 3D atmospheric structure and wind dynamics.

712

713 **[Figure 9]**

714

715 *4.2.3 Special case of Xanadu*

716

717 Apart from its wavy pattern, one of the most striking structures of the longitudinal
718 distribution of mid-latitude clouds is the very low cloud fractional coverage, below 5% on
719 average, regularly found in the vicinity of -90°E longitude between 2003 and 2010 (see
720 **Figure 9b, 9c**, and curves of the **Figure 9d**), interrupting the continuity of the mid-latitude
721 cloud belt (see the global map of Titan in **Figure 10**). This region of very poor cloud activity,
722 ~50° wide in longitudes, lies right above the southern part of the peculiar Titan surface feature

723 called Xanadu (see **Figures 9a and 10**). Contrary to what was previously proposed
724 (Adamkovics et al., 2007, 2009), we do not see any evidence in our data for an enhancement
725 of methane condensation, precipitation or drizzle over Xanadu. Our long-term observations
726 show that Xanadu seems to act more as an “obstacle” to cloud formation than a privileged
727 area for condensation. Preferential condensation of methane right above Xanadu was
728 previously contested by Kim et al. (2008) arguing that the Adamkovics et al. (2007) analysis
729 was biased by surface artifacts.

730

731 **[Figure 10]**

732

733 In many respects, Xanadu is one of the most remarkable regions of Titan. Even from Earth-
734 based telescopic observations, Xanadu is known to be among the brightest areas of the moon
735 in the near-infrared, in the 0.93-2 μm range (Lemmon et al., 1993; Smith et al., 1996; Gibbard
736 et al., 1999; Coustenis et al., 2001). The Cassini RADAR images of Xanadu revealed that
737 most of the ~ 5 million km^2 area is dominated by extended mountain ranges that are thought to
738 originate from Titan’s large scale tectonism (Radebaugh et al., 2007, 2011). The uniqueness
739 of this region is also noticeable from the Cassini RADAR radiometry experiment (Janssen et
740 al., 2009). This is the only region of Titan to have such a combination of low emissivity, low
741 dielectric constant (almost unity) and high volume scattering at 2.2-cm wavelength. It was
742 interpreted as an area whose surface is globally covered by fractured ice largely overlain by a
743 fluffy material. Long thought to be an elevated continent, recent altimetry investigations
744 showed however that Xanadu is rather a large smooth depression, ~ 1 km deeper than the
745 average geoid (Zebker et al., 2009).

746 Albedo and topography may significantly impact the atmospheric circulation and local
747 meteorology. The effects of surface brightness and large-scale topography were examined by

748 Tokano (2008) with the Cologne 3D GCM for Titan. They showed that the presence of
749 Xanadu may markedly perturb the regional patterns of near-surface winds. In particular, if
750 Xanadu is a large basin with a relative high albedo, they predict that the wind should then arc
751 clockwise north of Xanadu and anti-clockwise west and south of Xanadu, in agreement with
752 the dune orientations in the vicinity of Xanadu. According to this model, incoming westerlies
753 are ejected outside of Xanadu and become stronger and more unidirectional than inside
754 Xanadu, leaving Xanadu's inside wind more erratic and quieter. It is possible that such large-
755 scale near-surface wind perturbations generated by Xanadu may also impact the regional
756 transport of humidity. The strong surrounding winds may cast the local humidity outside the
757 boundaries of Xanadu, and therefore dry up the air inside regions of Xanadu and somewhat
758 inhibit the cloud formation in this region. An alternative or complementary mechanism may
759 be also invoked. If we consider again that Xanadu is a depression (Zebker et al., 2009), then
760 the air that enters Xanadu and flows downward its slopes would adiabatically warm,
761 contributing to the reduction of its relative humidity and suppressing cloud formation. These
762 mechanisms need to be investigated by GCMs which include 3D atmospheric and cloud
763 structure, wind dynamics and topography.

764

765 **5. Conclusions**

766

767 We have presented here the complete monitoring of cloud activity in Titan's atmosphere
768 between July 2004 and April 2010, as observed by the VIMS instrument onboard the Cassini
769 spacecraft. This 6-year long period covers northern winter up to early northern spring,
770 including the equinox in August 2009. We developed a semi-automated algorithm to detect
771 cloud contribution within the VIMS dataset and produced maps of the cloud coverage for
772 each of the Cassini flybys of Titan, and derived the latitudinal and longitudinal distributions

773 of the clouds and their evolution with time. The persistence, location, and periodicity of the
774 clouds were compared with the forecast of the General Circulation Models (GCMs) (Rannou
775 et al., 2006; Mitchell et al., 2006, 2009). These new constraints, along with ground-based
776 observations, can contribute to the refinements of GCMs predictions and to a better
777 understanding of Titan's climate.

778 Between 2004 and 2008 (i.e., late northern winter), we show that Titan's meteorology was
779 very stable: 1) a widespread and long-lived cloud capped the entire northern polar vortex
780 region, poleward of 60°N; apart from the polar cloud, the northern hemisphere (winter
781 hemisphere) was entirely cloud-free, and 2) sporadic clouds were regularly seen at mid-
782 latitudes and above the pole in the southern hemisphere (summer hemisphere). Our
783 observations support the interpretation that the winter (northern) polar cloud is caused by the
784 sinking and cooling of stratospheric air into the colder troposphere and the preferential
785 condensation of droplets of ethane, and that the summer (southern) stormy clouds are more
786 likely convective in nature and mainly composed of methane droplets. The latitudinal
787 clustering of the clouds and the hemispheric asymmetry of their physical and chemical
788 properties are both satisfactorily predicted by the GCMs.

789 After mid-2008, we observed the first strong evidence of a global decline of Titan's cloud
790 activity. At the end of 2008, the clouds at the south pole disappeared. At the same time, the
791 northern polar cloud began to show clear signs of fragmenting, finally to completely vanish
792 after the equinox as predicted by the IPSL-TGCM (Rannou et al., 2006). We also detected a
793 dozen cloud outbursts at the tropics, which seemed to be more frequent as equinox
794 approaches. All these observations show that we are likely witnessing the onset of the
795 seasonal pole-to-pole circulation turnover on Titan. The meteorology is then expected to
796 completely reverse from one hemisphere to another in the next 5 or 6 terrestrial years, as
797 predicted by the models. The persistence of southern mid-latitude clouds at 40°S through mid-

798 2010, and the occurrence, a few months before and after the equinox, of more frequent
799 equatorial clouds along with first appearance of northern mid-latitude clouds seem to suggest
800 rather an abrupt hemispherical reversal of cloud activity, even if these equatorial and northern
801 mid-latitude events are still too rare to be fully significant. The Cassini Solstice Mission will
802 observe Titan up to the beginning of northern summer, in 2017, and should help to
803 definitively solve the question of the meteorological hemispheric reversal, and the question of
804 the type of atmospheric circulation (symmetric or asymmetric).

805 We also analyzed the longitudinal distribution of southern clouds at the time they were
806 active. We found a prominent structure in the longitudinal distribution of clouds at southern
807 high-latitudes that can be attributed to the presence of Ontario Lacus, the largest hydrocarbon
808 reservoir in the region. As well, we observed that the southern mid-latitude clouds are
809 distributed with an $n=2$ -mode wave pattern with peaks at 0° and $\sim 180^\circ\text{E}$ longitudes. Very
810 stable with time, this pattern is interpreted to originate from Saturn's tides. In addition, we
811 noticed a constant deficit of clouds at $\sim 40^\circ\text{S}$ and $\sim 90^\circ\text{E}$, southward of Xanadu, which could
812 be related to the local perturbation of winds and cloud formation by the large scale
813 topography and high albedo of the Xanadu continent.

814 Areas significantly covered by clouds could also be interesting to observe as primary
815 targets with imaging systems (radar and optical instruments) in order to detect surface features
816 possibly related to rainfall events, or release of methane by subsurface processes or
817 cryovolcanic activity. Continuing observations during the Cassini Solstice Mission will
818 provide opportunities to investigate such phenomena.

819 Finally, our observation show that two-dimensional geometry for the GCMs must be
820 extended to a fully three-dimensional grid in order to fully apprehend the impact of highly
821 non-axisymmetric mechanisms on circulation and tropospheric cloud formation, such as the
822 diurnal cycle of Saturn's tides or the topography. A fully 3D model may be also required to

823 predict with more efficiency the haze and cloud microphysics and the seasonality of Titan's
824 clouds and/or precipitation.

825

826

827 **Acknowledgments**

828

829 This work benefited from financial support from the Centre National de la Recherche
830 Scientifique, Institut National des Sciences de l'Univers, from the French Centre National
831 d'Etudes Spatiales (CNES) and from the ANR (project Exoclimat). Part of this work was
832 performed at the Jet Propulsion Laboratory, California Institute of Technology, under contract
833 to the National Aeronautics and Space Administration. We gratefully acknowledge the long
834 years of work done by the entire Cassini and VIMS teams that allowed (and still allow) the
835 acquisition of these outstanding sets of data. We also thank the two anonymous reviewers for
836 very insightful comments and suggestions that helped the manuscript.

837

838 **References:**

839

840 Adamkovics, M., Wong, M.H., Laver, C., de Pater, I., 2007. Widespread Morning Drizzle on
841 Titan. *Science* 318, 962-965.

842

843 Adamkovics, M., de Pater, I., Hartung, M., Barnes, J.W., 2009. Evidence for condensed-phase
844 methane enhancement over Xanadu on Titan. *Planet. Space Sci.* 57, 1586-1595.

845

846 Aharonson, O., Hayes, A.G., Lunine, J.I., Lorenz, R.D., Allison, M.D., Elachi, C., 2009. An
847 asymmetric distribution of lakes on Titan as a possible consequence of orbital forcing. *Nature*
848 *Geoscience* 2, 851-854.
849
850 Atreya, S.K., et al., 2006. Titan's methane cycle. *Planet. Space Sci.* 54, 1177-1187.
851
852 Baines, K.H., et al., 2005. The Atmospheres of Saturn and Titan in the Near-Infrared First
853 Results of Cassini/VIMS. *Earth Moon Planet* 96, 119-147.
854
855 Barnes, J.W., et al., 2005. A 5-Micron-Bright Spot on Titan: Evidence for Surface Diversity.
856 *Science* 310, 92-95.
857
858 Barnes, J.W., et al., 2006. Cassini observations of flow-like features in western Tui Regio,
859 Titan. *Geophys. Res. Lett.* 33, CiteID L16204.
860
861 Barnes, J.W., et al., 2007. Global-scale surface spectral variations on Titan seen from
862 Cassini/VIMS. *Icarus* 186, 242-258.
863
864 Barnes, J.W., et al., 2008. Spectroscopy, morphometry, and photoclinometry of Titan's
865 dunefields from Cassini/VIMS. *Icarus* 195, 400-414.
866
867 Barnes, J.W., et al., 2009. VIMS spectral mapping observations of Titan during the Cassini
868 prime mission. *Planet. Space Sci.* 57, 1950-1962.
869

870 Barth, E.L., Rafkin, S.C.R., 2007. TRAMS: a new dynamic cloud model for Titan's methane
871 clouds. *Geophys. Res. Lett.* 34. doi:10.1029/2006GL028652.
872

873 Bouchez, A.H., Brown, M.E., 2005. Statistics of Titan's south polar tropospheric clouds.
874 *Astrophys. J.* 618, L53–L56.
875

876 Brown, M.E., Bouchez, A.H., Griffith, C.A., 2002. Direct detection of variable tropospheric
877 clouds near Titan's south pole. *Nature* 420, 795–797.
878

879 Brown, M.E., et al., 2009. Discovery of lake-effect clouds on Titan. *Geophys. Res. Lett.* 36,
880 CiteID L01103.
881

882 Brown, M.E., Roberts, J.E., Schaller, E.L., 2010. Clouds on Titan during the Cassini prime
883 mission: A complete analysis of the VIMS data. *Icarus* 205, 571-580.
884

885 Brown, R.H., et al., 2004. The Cassini Visual and Infrared Mapping Spectrometer
886 investigation. *Space Sci. Rev.* 115, 111–168.
887

888 Brown, R.H., et al., 2008. The identification of liquid ethane in Titan's Ontario Lacus. *Nature*
889 454, 607-610.
890

891 Coustenis, A., et al., 2001. Images of Titan at 1.3 and 1.6 μm with adaptative optics at the
892 CFHT. *Icarus* 154, 501-515.
893

894 de Pater, I., et al., 2006. Titan imagery with Keck adaptive optics during and after probe entry.
895 J. Geophys. Res. 111, CiteID E07S05. doi:10.1029/2005JE002620.
896

897 Flasar, F.M., 1998. The composition of Titans atmosphere: a meteorological perspective.
898 Planet. Space Sci. 46, 1109-1124.
899

900 Fulchignoni, M., et al., 2005. In situ measurements of the physical characteristics of Titan's
901 environment. Nature 438, 785-791.
902

903 Gibbard, S.G., et al., 1999. Titan: high resolution speckle images from the Keck telescope.
904 Icarus 139, 189-201.
905

906 Gibbard, S.G., et al., 2004. Speckle imaging of Titan at 2 microns: surface albedo, haze
907 optical depth, and tropospheric clouds 1996-1998. Icarus 169, 429-439.
908

909 Griffith, C.A., Owen, T., Miller, G.A., Geballe, T.R., 1998. Transient clouds in Titan's lower
910 atmosphere. Nature 395, 575-578.
911

912 Griffith, C.A., Hall, J.L., Geballe, T.R., 2000. Detection of Daily Clouds on Titan. Science
913 290, 509-513.
914

915 Griffith, C.A., et al., 2005. The Evolution of Titan's Mid-Latitude Clouds. Science 310, 474-
916 477.
917

918 Griffith, C.A., et al., 2006. Evidence for a Polar Ethane Cloud on Titan. *Science* 313, 1620-
919 1622.
920
921 Griffith, C.A., et al., 2009. Characterization of Clouds in Titan's Tropical Atmosphere.
922 *Astrophys. J. Letters* 702, L105-L109.
923
924 Hayes, A.G., et al., 2010. Bathymetry and absorptivity of Titan's Ontario Lacus. *J. Geophys.*
925 *Res.* 115, CiteID E09009. doi:10.1029/2009JE003557.
926
927 Hirtzig, M., et al., 2006. Monitoring atmospheric phenomena on Titan. *Astron. Astrophys.*
928 456, 761-774.
929
930 Hirtzig, M., et al., 2007. Titan: Atmospheric and surface features as observed with Nasmyth
931 Adaptive Optics System Near-Infrared Imager and Spectrograph at the time of the Huygens
932 mission. *J. Geophys. Res.* 112, CiteID E02S91.
933
934 Hueso, R., Sanchez-Lavega, A., 2006. Methane storms on Saturn's moon Titan. *Nature* 442,
935 428-431.
936
937 Janssen, M.A., et al., 2009. Titan's surface at 2.2-cm wavelength imaged by the Cassini
938 RADAR radiometer: Calibration and first results. *Icarus* 200, 222-239.
939
940 Jennings, D.E., et al., 2009. Titan's surface brightness temperatures. *Astrophys. J.* 691, L103-
941 L105.
942

943 Lebonnois, S., Rannou, P., Hourdin, F., 2009. The coupling of winds, aerosols and chemistry
944 in Titan's atmosphere. *Phil. Trans. R. Soc. A* 367, 665–682. doi:10.1098/rsta.2008.0243.
945

946 Le Corre, L., et al., 2009. Analysis of a cryolava flow-like feature on Titan. *Planet. Space Sci.*
947 57, 870-879.
948

949 Lemmon, M.T., Karkoschka, E., Tomasko, M., 1993. Titan's rotation - Surface feature
950 observed. *Icarus* 103, 329-332.
951

952 Le Mouélic, S., et al., 2008a. Imaging of the north polar cloud on Titan by the VIMS imaging
953 spectrometer onboard Cassini. *Lunar Planet. Sci. XXXIX*, 1649 (abstract).
954

955 Le Mouélic, S., et al., 2008b. Mapping and interpretation of Sinlap crater on Titan using
956 Cassini VIMS and RADAR data. *J. Geophys. Res.* 113, CiteID E04003.
957

958 Le Mouélic, S., et al. Dissipation of Titan's north polar Cloud at northern spring equinox.
959 *Planet. Space Sci.*, in press.
960

961 Mace, G.G., et al., 2009. A description of hydrometeor layer occurrence statistics derived
962 from the first year of merged Cloudsat and CALIPSO data. *J. Geophys. Res.* 114, D00A26,
963 doi:10.1029/2007JD009755.
964

965 Mitchell, J.L., Pierrehumbert, R.T., Frierson, D.M.W., Caballero, R., 2006. The dynamics
966 behind Titan's methane clouds. *P. Natl Acad. Sci. USA* 103, 18421- 18426.
967

968 Mitchell, J.L., Pierrehumbert, R.T., Frierson, D.M.W., Caballero, R., 2009. The impact of
969 methane thermodynamics on seasonal convection and circulation in a model Titan
970 atmosphere. *Icarus* 203, 250-264.
971

972 Mitri, G., Showman, A.P., Lunine, J.I., Lorenz, R.D., 2007. Hydrocarbon lakes on Titan.
973 *Icarus* 186, 385–394.
974

975 Newman, C.E., Richardson, M.I., Lee, C., Toigo, A.D., Ewald, S.P., 2008. The TitanWRF
976 model at the end of the Cassini prime mission. American Geophysical Union, Fall Meeting,
977 abstract #P12A-02.
978

979 Porco, C.C., et al., 2004. Cassini imaging science: Instrument characteristics and anticipated
980 scientific investigations at Saturn. *Space Sci. Rev.* 115, 363-497.
981

982 Porco, C.C., et al., 2005. Imaging of Titan from the Cassini spacecraft. *Nature* 434, 159-168.
983

984 Radebaugh, J., et al., 2007. Mountains on Titan observed by Cassini Radar. *Icarus* 192, 77–
985 91.
986

987 Radebaugh, J., et al., 2011. Regional geomorphology and history of Titan’s Xanadu province.
988 *Icarus* 211, 672-685. doi:10.1016/j.icarus.2010.07.022.
989

990 Rannou, P., Montmessin, F., Hourdin, F., Lebonnois, S., 2006. The latitudinal distribution of
991 clouds on Titan. *Science* 311, 201–205.
992

993 Rannou, P., Cours, T., Le Mouélic, S., Rodriguez, S., Sotin, C., Drossart, P., Brown, R., 2010.
994 Titan haze distribution and optical properties retrieved from recent observations. *Icarus* 208,
995 850-867.
996
997 Rodriguez, S., et al., 2006. Cassini/VIMS hyperspectral observations of the HUYGENS
998 landing site on Titan. *Planet. Space Sci.* 54, 1510-1523.
999
1000 Rodriguez, S., et al., 2009. Global circulation as the main source of cloud activity on Titan.
1001 *Nature* 459, 678-682.
1002
1003 Roe, H.G., de Pater, I., Macintosh, B.A., McKay, C.P., 2002. Titan's Clouds from Gemini and
1004 Keck Adaptive Optics Imaging. *Astrophys. J.* 581, 1399-1406.
1005
1006 Roe, H.G., Bouchez, A.H., Trujillo, C.A., Schaller, E.L., Brown, M.E., 2005a. Discovery of
1007 Temperate Latitude Clouds on Titan. *Astrophys. J.* 618, L49-L52.
1008
1009 Roe, H.G., Brown, M.E., Schaller, E.L., Bouchez, A.H., Trujillo, C.A., 2005b. Geographic
1010 Control of Titan's Mid-Latitude Clouds. *Science* 310, 477-479.
1011
1012 Schaller, E.L., Brown, M.E., Roe, H.G., Bouchez, A.H., 2006a. A large cloud outburst at
1013 Titan's south pole. *Icarus* 182, 224-229.
1014
1015 Schaller, E.L., Brown, M.E.; Roe, H.G.; Bouchez, A.H.; Trujillo, C.A., 2006b. Dissipation of
1016 Titan's south polar clouds. *Icarus* 184, 517-523.
1017

1018 Schaller, E.L., Roe, H.G., Schneider, T., Brown, M.E., 2009. Storms in the tropics of Titan.
1019 Nature 460, 873-875.
1020
1021 Smith, P.H., Lemmon, M.T., Lorenz, R.D., Sromovsky, L.A., Caldwell, J.J., Allison, M.D.,
1022 1996. Titan's surface, revealed by HST imaging. Icarus 119, 336-349.
1023
1024 Soderblom, L.A., et al., 2007. Topography and geomorphology of the Huygens landing site
1025 on Titan. Planet. Space Sci. 55, 2015-2024.
1026
1027 Sotin, C., et al., 2005. Release of volatiles from a possible cryovolcano from near-infrared
1028 imaging of Titan. Nature 435, 786-789.
1029
1030 Stofan, E.R., et al., 2007. The lakes of Titan. Nature 445, 61-64.
1031
1032 Tokano, T., 2005. Meteorological assessment of the surface temperatures on Titan:
1033 Constraints on the surface type. Icarus 173, 222-242.
1034
1035 Tokano, T., 2008. Dune-forming winds on Titan and the influence of topography. Icarus,
1036 Volume 194, 243-262.
1037
1038 Tokano, T., 2009. Impact of seas/lakes on polar meteorology of Titan: Simulation by a
1039 coupled GCM-Sea model. Icarus 204, 619-636.
1040
1041 Tokano, T., Neubauer, F.M., 2002. Tidal winds on Titan caused by Saturn. Icarus 158, 499-
1042 515.

1043

1044 Tokano, T., Neubauer, F.M., 2005. Wind-induced seasonal angular momentum exchange at
1045 Titan's surface and its influence on Titan's length-of-day. *Geophys. Res. Lett.* 32, CiteID
1046 L24203.

1047

1048 Tokano, T., Neubauer, F.M., Laube, M. McKay, C.P., 2001. Three-Dimensional Modeling of
1049 the Tropospheric Methane Cycle on Titan. *Icarus* 153, 130-147.

1050

1051 Tomasko, M.G., et al., 2005. Rain, winds and haze during the Huygens probe's descent to
1052 Titan's surface. *Nature* 438, 765-778.

1053

1054 Toublanc, D., Parisot, J.-P., Brillet, J., Gautier, D., Raulin, F., McKay, C.P., 1995.
1055 Photochemical modeling of Titan's atmosphere. *Icarus* 113, 2-26.

1056

1057 Turtle, E.P., et al., 2009. Cassini imaging of Titan's high-latitude lakes, clouds, and south-
1058 polar surface changes. *Geophys. Res. Lett.* 36, CiteID L02204.

1059

1060 Yung, Y.L., Allen, M., Pinto, J.P., 1984. Photochemistry of the atmosphere of Titan -
1061 Comparison between model and observations. *Astrophys. J. Suppl. Series* 55, 465-506.

1062

1063 Wall, S., et al., 2010. Active shoreline of Ontario Lacus, Titan: A morphological study of the
1064 lake and its surroundings. *Geophys. Res. Lett.* 37, CiteID L05202.

1065

1066 Zebker, H.A., Stiles, B., Hensley, S., Lorenz, R., Kirk, R.L., Lunine, J.I., 2009. Size and
1067 Shape of Saturn's Moon Titan. *Science* 324, 921- 923.

1068 **Appendix: Comparison between Rodriguez et al. (2009) and Brown et al. (2010) Titan's**
1069 **clouds surveys**

1070

1071 Brown et al. (2010) also analyzed the VIMS dataset with the same objective as Rodriguez et
1072 al. (2009) to map Titan's cloud occurrences during the Cassini prime mission. Brown et al.
1073 (2010) study extended the monitoring of Titan's clouds up to July 2008. Significant
1074 discrepancies with the study of Rodriguez et al. (2009) were pointed out.

1075 For every ~9000 spectro-images of the nominal mission VIMS dataset, Brown et al. (2010)
1076 construct a set of three synthetic images referenced in their work as the "surface",
1077 "troposphere" and "stratosphere" images by combining VIMS channels only sensitive to
1078 Titan's surface, tropospheric and stratospheric features respectively. Each of the ~9000
1079 triplets of images is visually inspected to search for clouds that appear in the surface and
1080 troposphere images but not in the stratosphere image. Finally for each of the images identified
1081 as having clouds, they hand-select all image pixels that contain a cloud, making a map of
1082 observed clouds on Titan for each image.

1083 **Table A1** presents the synthesis of each cloud detected in the VIMS dataset between July
1084 2004 and July 2008 (Brown et al., 2010), July 2004 and December 2007 (Rodriguez et al.,
1085 2009) and January 2008 and April 2010 (this work). The location and the condition of
1086 observation of these cloud events is specified each time they are available. During the
1087 nominal mission, by merging all the studies from July 2004 to July 2008, a total of 163
1088 individual cloud systems have been detected.

1089 All these detections have been thoroughly reexamined by re-analyzing the entire VIMS
1090 dataset between July 2004 and July 2008. The fact is that any cloud detection technique has
1091 limitations because most of the time there is a continuum of I/F values rather than a clear
1092 separation between surface and cloud spectra. However, in order to be as accurate and

1093 objective as possible, we decide to conduct this reexamination by jointly taking advantage of
1094 the semi-automated source separation method (Rodriguez et al., 2009) and the use of the pure
1095 visual inspection of relevant VIMS channels (Brown et al. (2010)). We thus performed a
1096 systematic re-analysis of each individual VIMS image by using simultaneously the
1097 ‘objectivity’ of the source separation technique and the ‘sensitivity’ of the tropospheric filter
1098 defined in Brown et al. (2010): cloud detection is ruled out if nothing is visible in the single
1099 2.1 μm band and in the tropospheric filter, and if at the same time no specific feature can be
1100 isolated in the 2D scatterplot of the 2.75 vs. 5- μm window integrated areas; on the contrary, if
1101 any feature shows up in the 2.1 band or tropospheric filter, or if the corresponding 2D
1102 scatterplot shows pixels isolated from the rest in the 2.75 and 5- μm high-value regions, the
1103 VIMS image is carefully considered and the feature is geographically isolated and thoroughly
1104 examined for cloud detection. A double independent and blind visual cross-checking of each
1105 new detection map thus produced, is then performed to further minimize the subjectivity and
1106 decide as firmly as possible between a robust detection and a rejection.

1107 The detailed reexamination of the complete VIMS dataset shows that Rodriguez et al.
1108 (2009) missed 20 confirmed clouds (12.3% of total), have shape problems with 6 clouds
1109 (3.7% of total) and uncertainly detect 5 clouds (3.1% of total). More than 93% of the 143
1110 Rodriguez et al. (2009) detections are therefore confirmed in terms of shape and location. The
1111 main drawback of the semi-automated routine of Rodriguez et al. (2009) is its lack of
1112 sensitivity in detecting the faintest clouds. This difficulty was previously identified and
1113 clearly stated in Rodriguez et al. (2009), due to the deliberate choice of conservative
1114 thresholds of detection. The consequences on the global mapping of Titan’s clouds over 3.5
1115 years including more than 140 cloud detections are minor and, in the end, this does not
1116 change any of the conclusions of Rodriguez et al. (2009) study. During this checking process,
1117 we also found a few systematic errors in the manual detection of Brown et al. (2010). In

1118 particular, we found that they missed 9 clouds (5.5% of total), and that their manual selection
1119 overestimates the spatial extent of 9 clouds (5.5% of total) and, on ten occasions, merges
1120 numerous small individual clouds into a larger unique event (equivalent of missing 19 other
1121 clouds (11.6% of total)). We also found 19 (11.6% of total) false or uncertain detections. At
1122 the end, ~80% of the 135 Brown et al. (2010) detections are found to be accurate both in
1123 shape and location. The method used by Brown et al. (2010) is more sensitive than the one of
1124 Rodriguez et al. (2009), as it allows them to miss fewer clouds. At the same time it appears to
1125 be too sensitive due to the inherent subjectivity of a pure visual inspection. The details of each
1126 detection consistency are given in **Table A1**. We can thus confirm 139 of the total 163
1127 detections (a total of 163 minus 5 and 19 uncertain detections from Rodriguez et al. (2009)
1128 and Brown et al. (2010) respectively). This finally gives a rate of good detections of 95%
1129 ($[143-6-5]=132$ over 139 confirmed clouds) for the semi-automated survey of Rodriguez et al.
1130 (2009) and 77% ($[135-9-19]=107$ over 139 confirmed clouds) for the visual examination of
1131 Brown et al. (2010), proving the quality of the two studies. Moreover, more than 75% of the
1132 total 163 clouds referenced in **Table A1** between July 2004 and July 2008 are jointly detected
1133 by Brown et al. (2010) and Rodriguez et al. (2009), indicating that both studies are very close.
1134 Both studies produced at the end almost the same global distribution and time evolution of the
1135 cloud coverage.

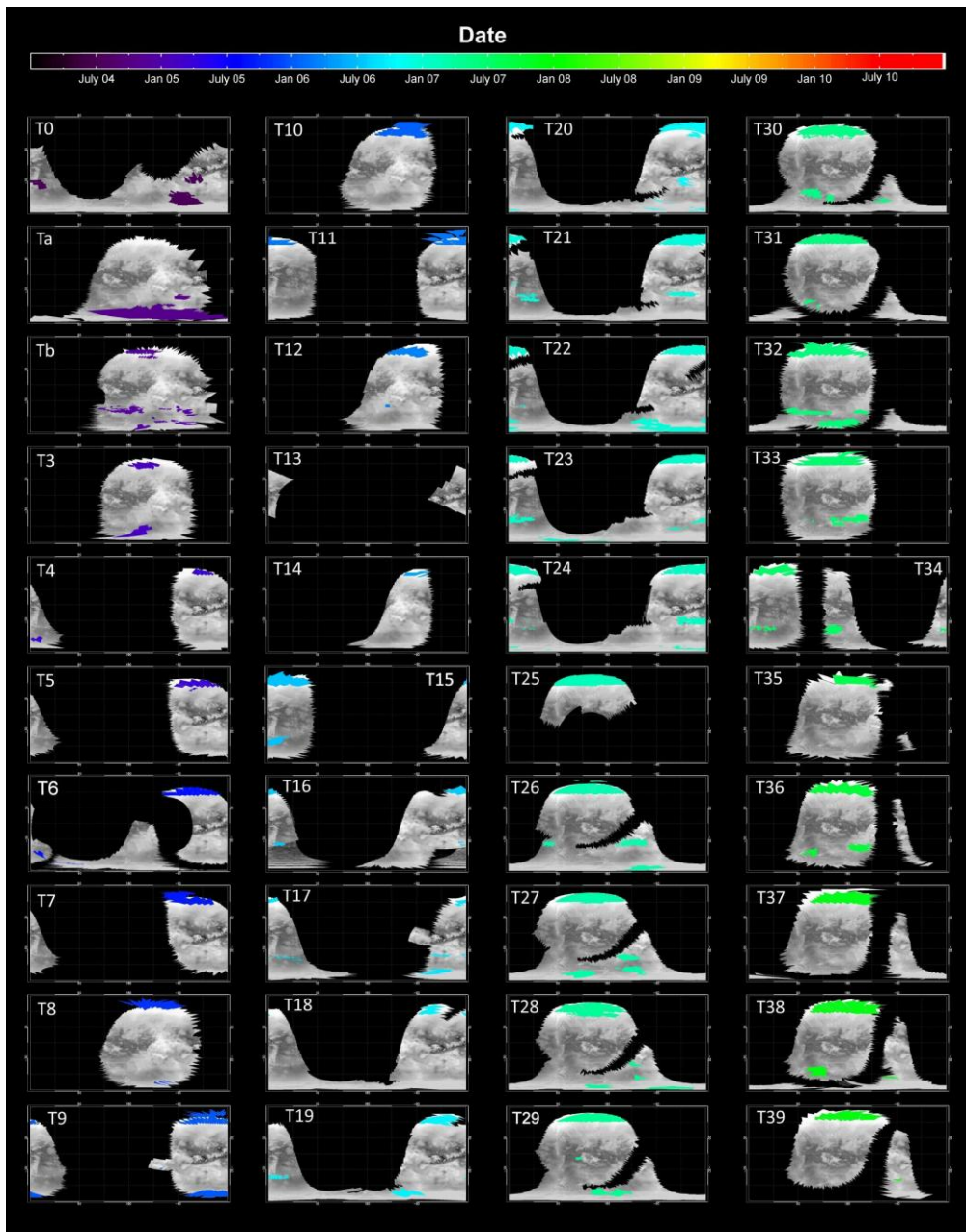
1136 We also notice that Figure 6 in Brown et al. (2010) is misleading. The cluster of VIMS
1137 flybys of Titan between October 2004 and January 2006 that they show in this figure is
1138 wrong. During this period, Cassini flew by Titan eight times, against only six in Brown et al.
1139 (2010) figure. Moreover a cluster of 5 targeted flybys between October 2004 and April 2005
1140 is erroneously shifted by six months in Brown et al. (2010) figure. By correcting all these
1141 errors, the Figure 6 of Brown et al. (2010) becomes very similar to the Figure 3a of Rodriguez
1142 et al. (2009) which also illustrates the time evolution of cloud latitude.

1143 It should be noted that the algorithm developed by Rodriguez et al. (2009) to detect Titan's
1144 clouds has the advantage of producing identical results every time, given the same dataset
1145 and detection criteria.

1146

1147 **[Table A1]**

1148

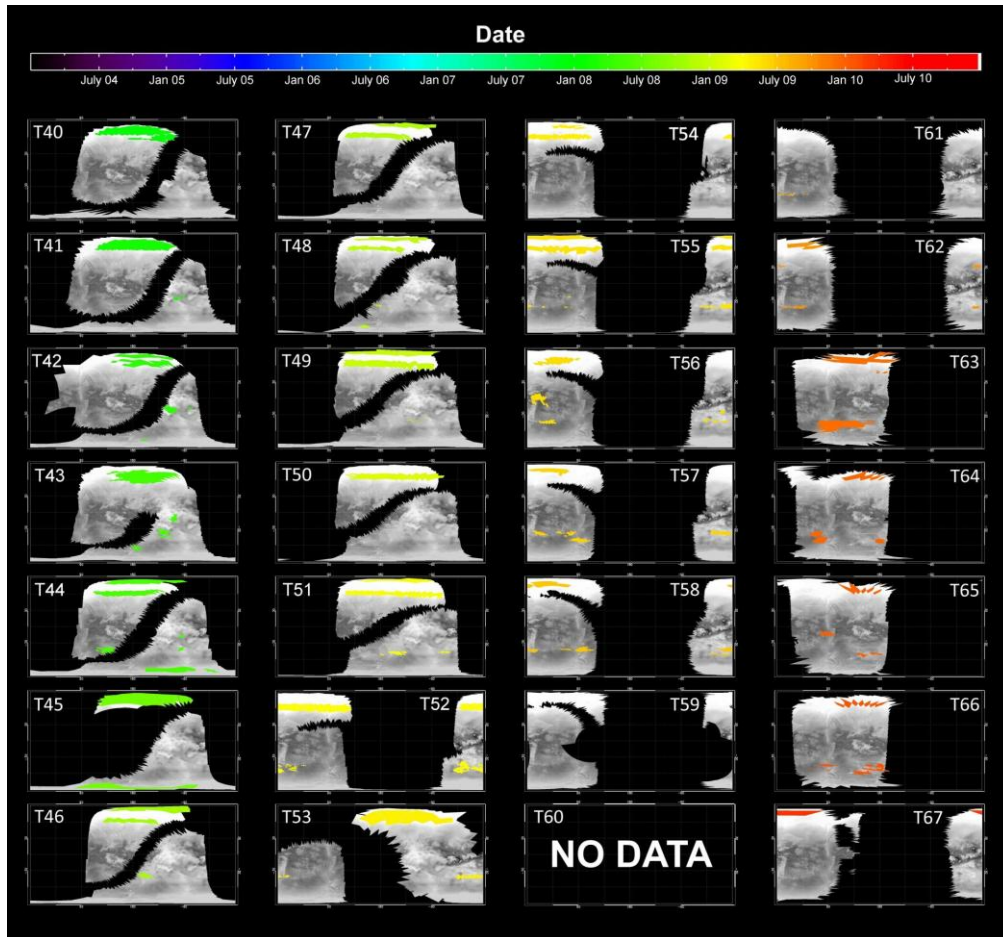


1150

1151 **Figure 1:** Maps of clouds observed by VIMS onboard Cassini during each of the 67 Titan
 1152 planned flybys from July 2004 (T0) until April 2010 (T67). The mapping projection is
 1153 rectangular with grid marks every 45° of longitude and 30° of latitude (0° longitude is on the
 1154 left). Longitude is in degrees east. A VIMS map of the observed areas is used as background
 1155 for each flyby. The resolution of the projection maps are of 0.3° in longitude and latitude (~14
 1156 km per pixel at the equator). Cloud detections are marked on each map with a rainbow color

1157 coding corresponding to the period they were observed (the precise flyby dates are referenced
1158 in **Table A1** of the **Appendix**).

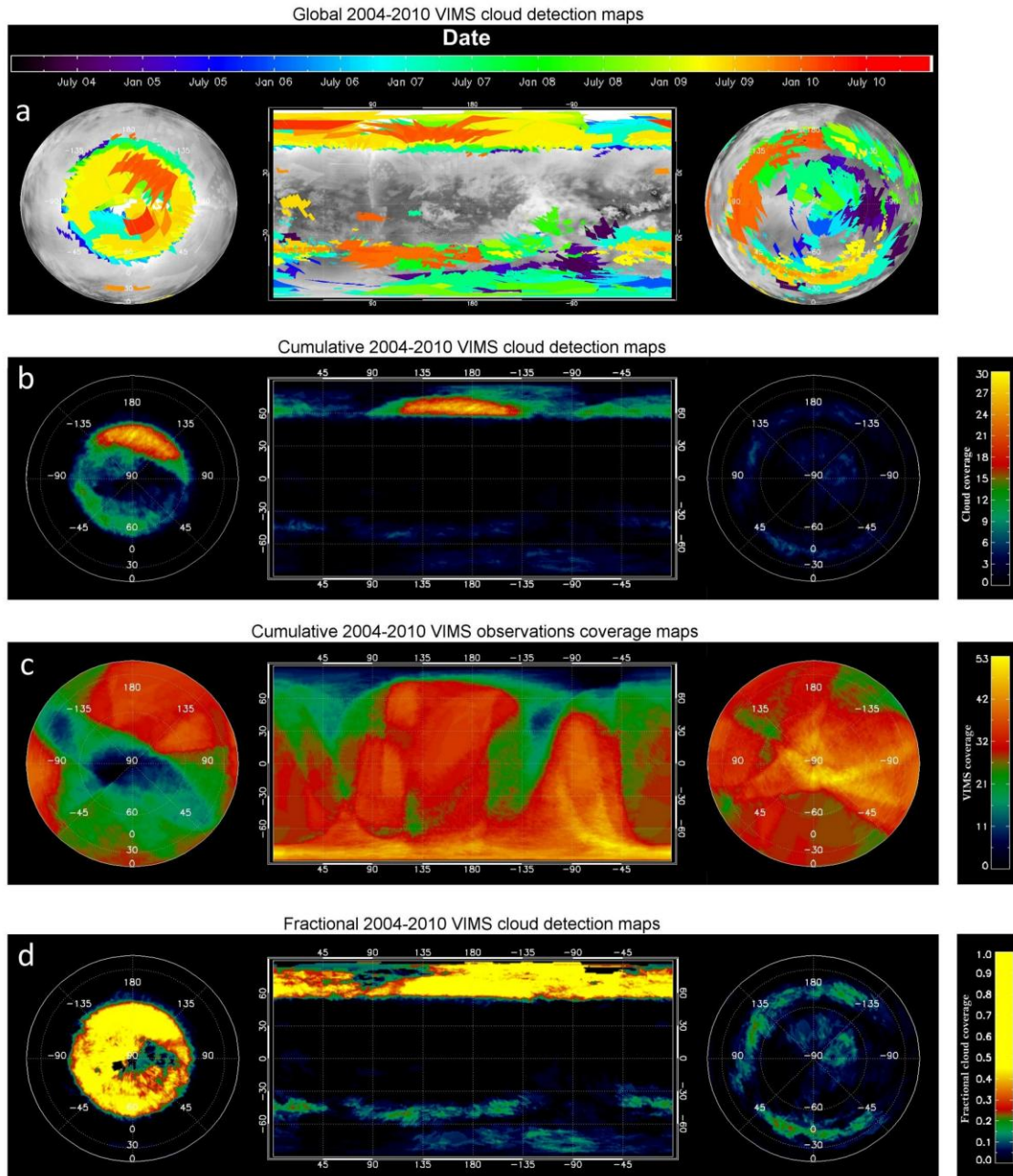
1159



1160

1161 **Figure 1:** (continued)

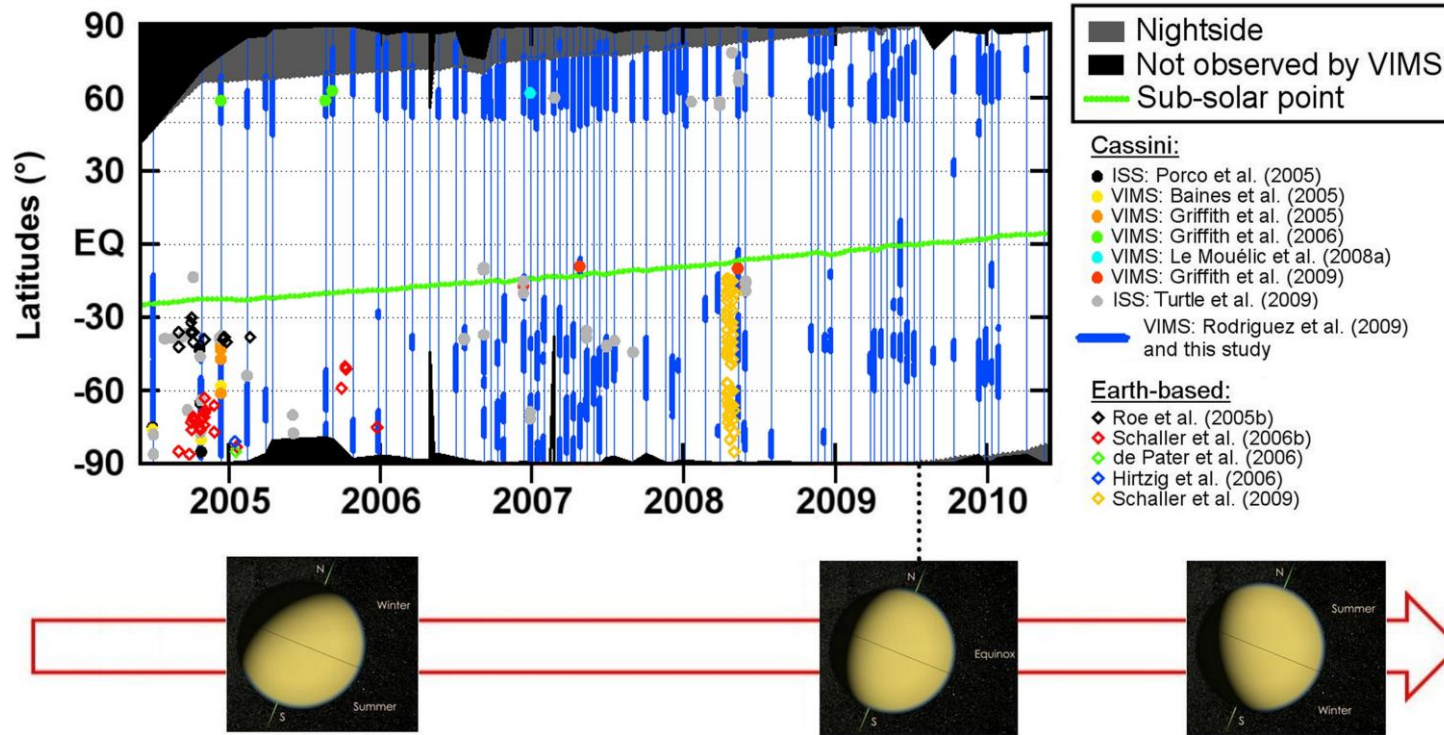
1162



1163

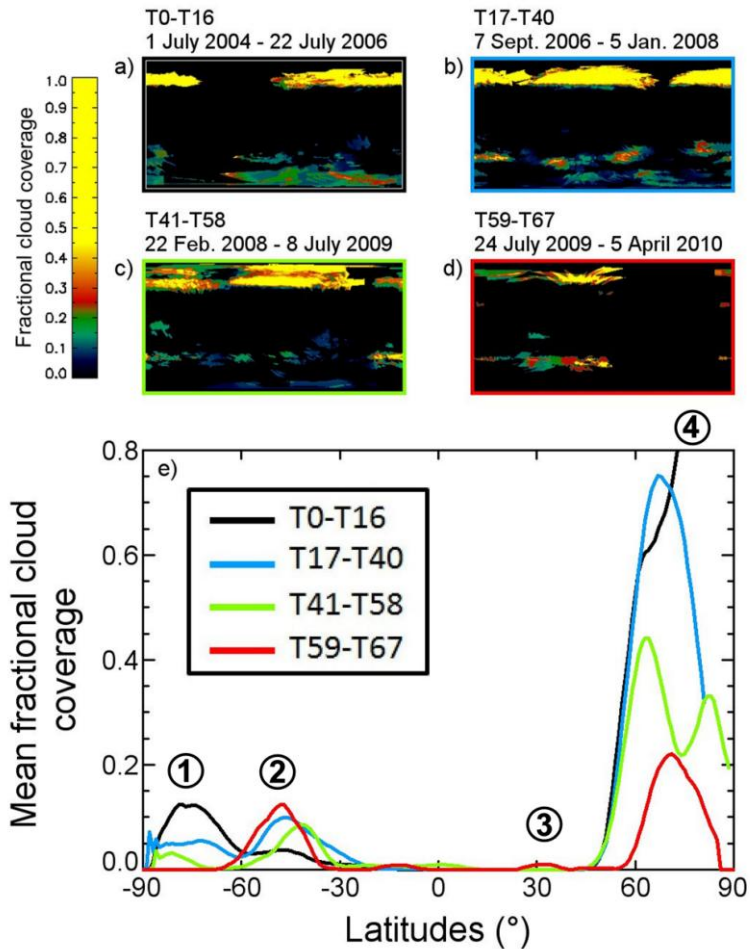
1164 **Figure 2:** (a) Synthesis of the cloud detections made by VIMS/Cassini between July 2004
 1165 and April 2010. The rectangular projection (middle), the basemap and the color coding are
 1166 similar to those of **Figure 1**. For the northern (left) and southern (right) polar projections, grid
 1167 marks are shown every 45° of longitude and 30° of latitude (0° longitude is down). Longitude
 1168 is in degrees east. (b) Cumulative number of clouds detected by VIMS in the 2004-2010
 1169 period. The color scale shows the number of times that a cloud was observed at each location.
 1170 (c) Coverage of VIMS observations in the 2004-2010 period. The color scale shows the

1171 number of flybys during which each point of Titan was imaged by VIMS with an incidence
1172 angle lower than 90° . **(d)** Fractional cloud coverage in the 2004-2010 period is obtained by
1173 dividing (b) by (c). The color scale saturates at 0.45 to enhance the southern cloud distribution
1174 and equatorial transient events. The fractional coverage in clouds of the north polar region
1175 exceeds 0.7 almost everywhere poleward of 60°N . The clouds of Titan mainly cluster at three
1176 distinct latitudes during the course of southern summer and at the beginning of southern fall:
1177 poleward of 60°N , poleward of 60°S and at $\sim 40^\circ\text{S}$. The resolution of all the rectangular and
1178 polar projections shown here are similar to those of **Figure 1** (0.3° corresponding to ~ 14 km
1179 per pixel at the equator).



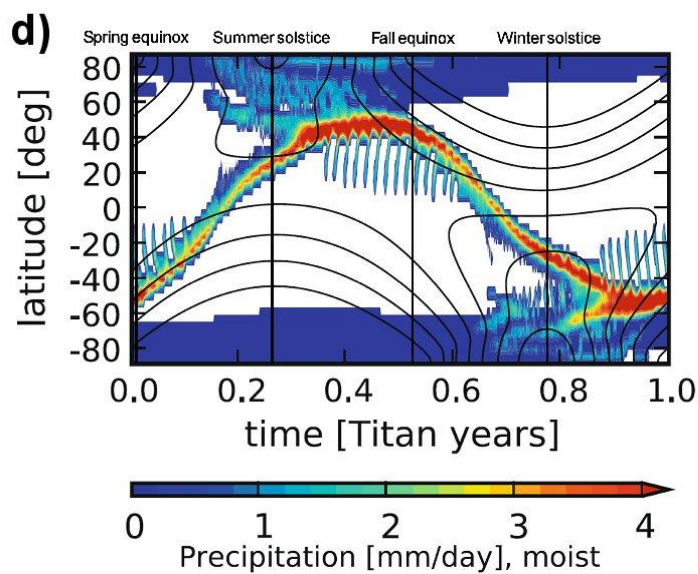
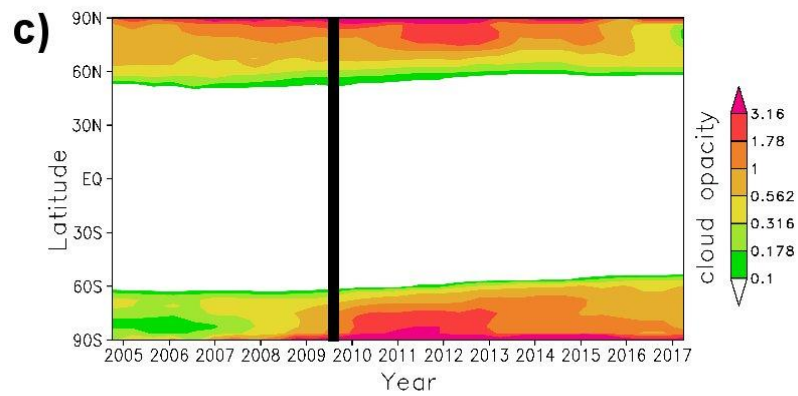
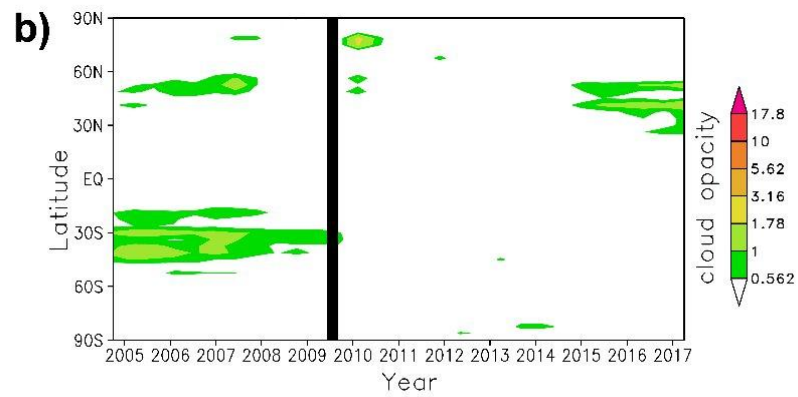
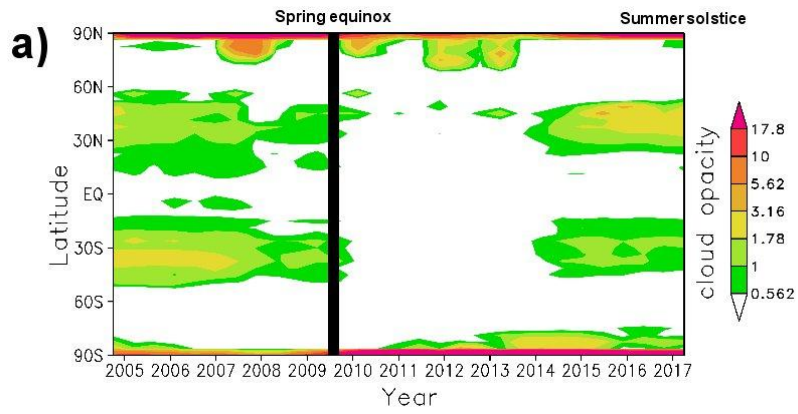
1180

1181 **Figure 3:** The latitudinal coverage of Titan's cloud activity with time between July 2004 and April 2010. Each thin blue vertical solid line marks
 1182 the time of Cassini flyby of Titan as well as the latitude coverage of the VIMS observations. The larger blue lines show the latitude extension of
 1183 clouds that we detected with VIMS, summed over all longitudes. Our detections are in very good agreement with previous Cassini (colored dots)
 1184 or Earth-based (colored diamonds) observations. The green line shows the latitude of the sub-solar point indicating the region of the maximum of
 1185 solar insolation. Northern spring equinox occurred in August 2009. At that time, the solar maximum was at the equator. (Credits for the views of
 1186 Titan seasonal illumination: © Animea, F. Durillon).



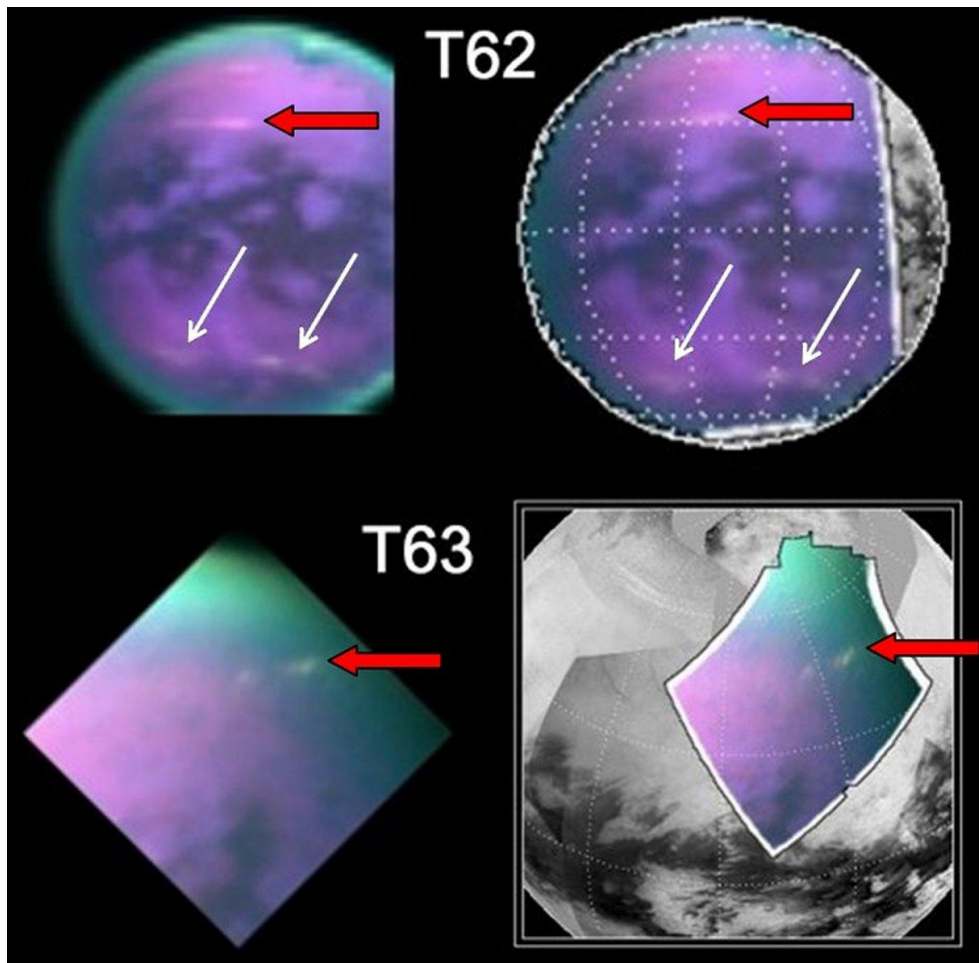
1187

1188 **Figure 4:** (a) to (d) Maps of fractional cloud coverage on Titan for four successive periods
 1189 (July 2004-July 2006, September 2006-January 2008, February 2008-July 2009, July 2009-
 1190 April 2010), using the same conventions as in **Figure 1**. The time resolution is slightly
 1191 sharper for the last two periods as they are closer to the equinox. (e) The corresponding
 1192 fractional cloud coverage as a function of latitude for the four periods considered in **Figures**
 1193 **4a-d**. The latitudinal fractional cloud coverage curves are obtained by averaging the fractional
 1194 cloud coverage maps (a)-(d) over longitudes. These distributions are all smoothed by a 10°
 1195 boxcar smoothing. Encircled numbers indicate particular regions of interest: ① and ④, the
 1196 south and north polar regions respectively, showing a drastic decline of cloud activity, ② the
 1197 southern mid-latitudes with a rather constant high activity (even after the equinox as shown
 1198 by the red line), and ③, the northern mid-latitudes with signs of very sporadic cloud activity
 1199 beginning here around equinox.



1201 **Figure 5: (a), (b) and (c)** Maps of Titan's cloud opacity, averaged over 5 consecutive years,
1202 between the ground and the pressure level 400 mbar (~23 km altitude), showing the coverage
1203 of methane clouds **(a)** and ethane clouds **(b)**, and above 400 mbar showing only the ethane
1204 clouds **(c)**, as predicted by the atmospheric global circulation model of Rannou et al. (2006)
1205 (IPSL-TGCM), between 2004 and 2017. In these simulations, the methane condensates
1206 dominate the opacity below 400 mbar and the model shows that the large and sporadic cloud
1207 structures seen at mid-latitude and very near the poles are due to methane **(a and b)**. On the
1208 other hand, the upper layer of cloud **(c)** is dominated near the poles by ethane condensate
1209 (with the north polar cloud thicker than the southern one in 2006). No methane cloud is
1210 produced above 400 mbar in these simulations. Although it remains less opaque than the low
1211 altitude methane cloud, the ethane cloud is best observed from orbit in the northern region
1212 because it is well above the methane condensation altitude. Note that these maps give the
1213 main structure of the cloud layer, but they are made from simulations which are not optimized
1214 to fit the most recent Cassini-Huygens observations. **(d)** Predictions of methane precipitations
1215 in Titan troposphere for an entire Titan's year from the Mitchell et al. (2009) GCM (directly
1216 taken from figure 6c of Mitchell et al. (2009)). The precipitation rate is averaged over 10-
1217 Titan-day. The black curves illustrate the pattern of solar forcing at the surface. Readers can
1218 refer to the text for a detailed comparison between our observations and the predictions of
1219 both GCMs.

1220

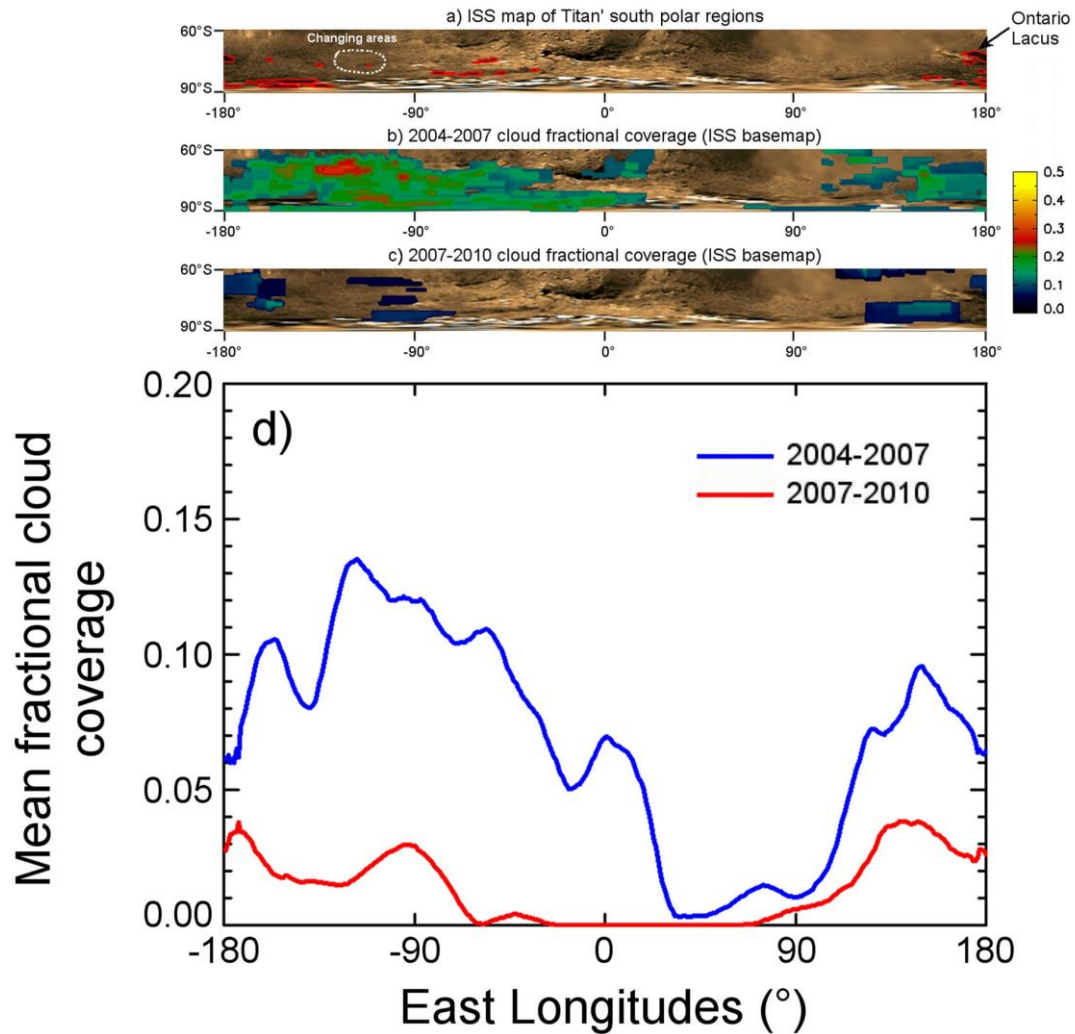


1221

1222 **Figure 6:** First occurrences of northern mid-latitude clouds (red arrows) after Titan's
 1223 equinox, at T62 (12 October 2009) and T63 flybys (12 December 2009). Raw (left) and
 1224 orthographically reprojected VIMS images (right) are color composite using the 5- μ m
 1225 channel as red, the 1.6- μ m as green and the 1.27- μ m as blue. Clouds show up as bright
 1226 elongated streaks. Southern mid-latitude clouds (white arrows) were still active at that time
 1227 (see T62 – left).

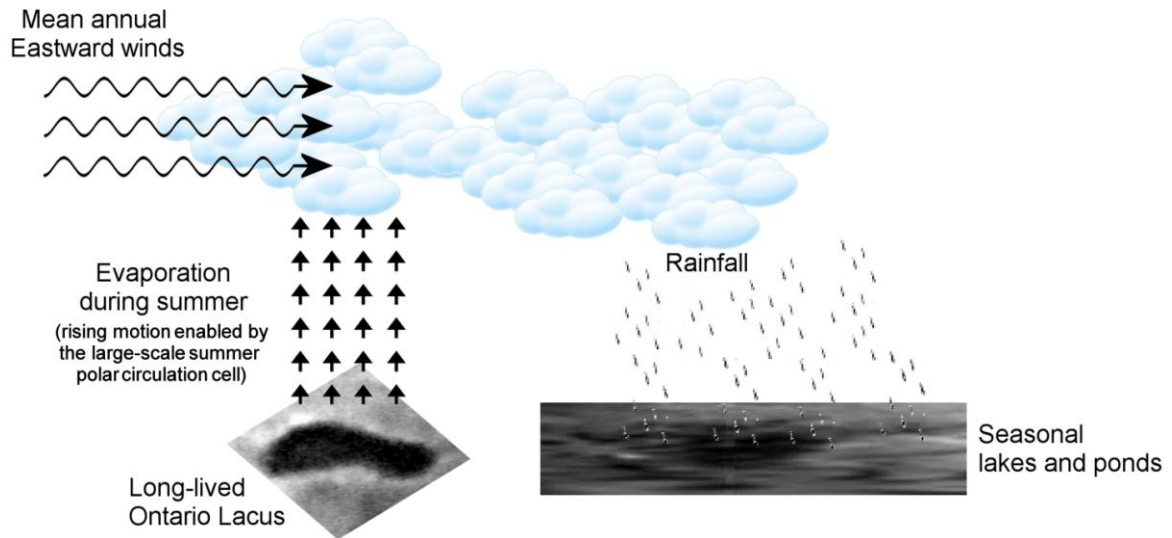
1228

1229



1230

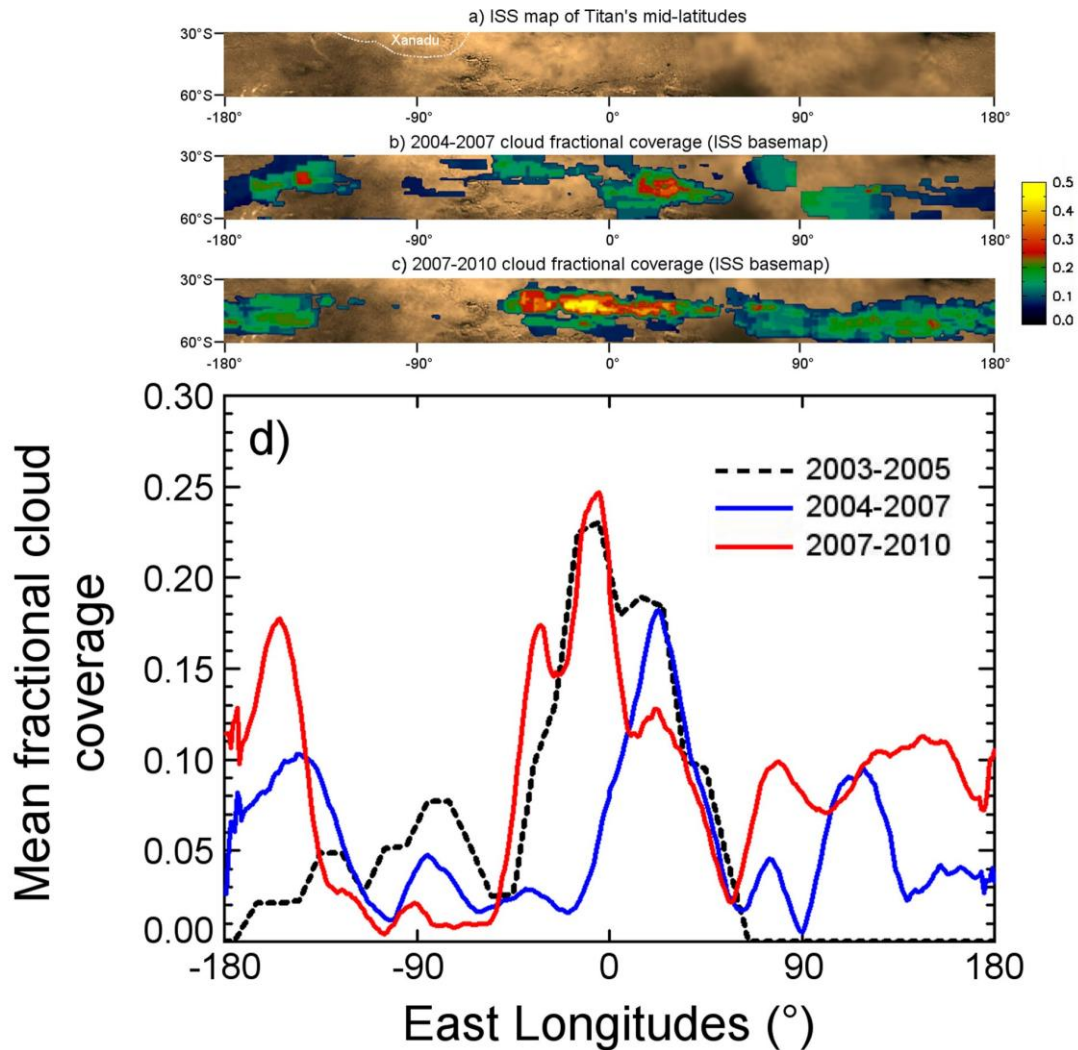
1231 **Figure 7:** (a) ISS rectangular map of Titan's southern region between 60°S
 1232 (colored from the grayscale map available at <http://www.ciclops.org/>). Ontario Lacus,
 1233 centered at 180°E and 70°S, as well as other small areas potentially filled with liquids (as
 1234 identified by Turtle et al., 2009) are outlined in red. The region where Turtle et al. (2009)
 1235 identified evidences of surface darkening between 2004 and 2005 is outlined with the white
 1236 dotted line. (b) Same ISS map of Titan overlapped by the 2004-2007 (from T0 up to T30
 1237 flyby) cloud fractional coverage. (c) ISS map of Titan overlapped by the 2007-2010 (from
 1238 T31 up to T67 flyby) cloud fractional coverage. (d) Fractional cloud coverage as a function of
 1239 longitudes, averaged between 60°S and 90°S, for the 2004-2007 (blue curve) and 2007-2010
 1240 (red curve) periods. These distributions are both smoothed by a 15° boxcar smoothing.



1241

1242 **Figure 8:** Possible scenario invoking a local methane cycle and zonal winds occurring at
 1243 southern high latitudes during the summer season. This scenario could explain the preferential
 1244 distribution of clouds eastward of Ontario Lacus (see **Figure 7**) and the surface changes
 1245 reported by the ISS instrument between 2004 and 2005 (Turtle et al., 2009).

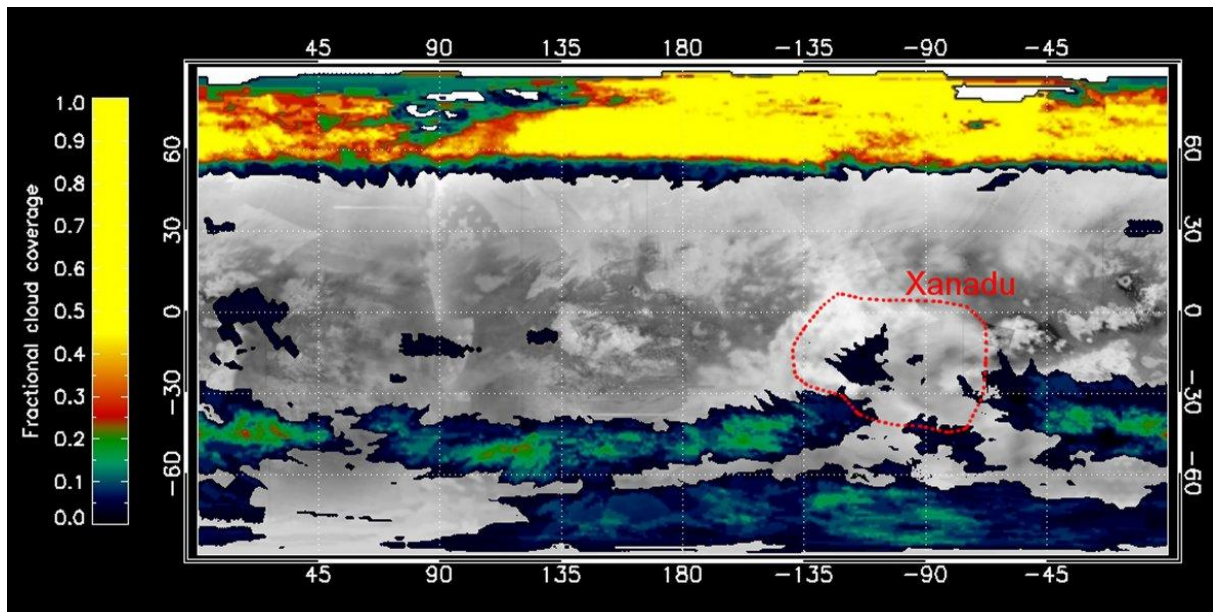
1246



1247

1248 **Figure 9:** (a) ISS rectangular map of Titan's mid-latitudes between 30°S and 60°S (colored
 1249 from the grayscale map available at <http://www.ciclops.org/>). The southern part of
 1250 Xanadu is outlined with the white dotted line. (b) Same ISS map of Titan overlapped by the
 1251 2004-2007 (from T0 up to T30 flyby) cloud fractional coverage. (c) ISS map of Titan
 1252 overlapped by the 2007-2010 (from T31 up to T67 flyby) cloud fractional coverage. (d)
 1253 Fractional cloud coverage as a function of longitudes, averaged between 35°S and 55°S, for
 1254 the 2004-2007 (blue curve) and 2007-2010 (red curve) periods. These distributions are both
 1255 smoothed by a 15° boxcar smoothing. The distribution reported by Roe et al. (2005b) from
 1256 telescopic observations between 2003 and 2005 is also shown in black dashed line.

1257



1258

1259 **Figure 10:** 2004-2010 fractional cloud coverage map overlapping the VIMS map of Titan
 1260 (similar to the one used in **Figures 1 and 2a**). The Xanadu region is outlined with a dotted red
 1261 line. The southern part of Xanadu shows clear evidences of cloud deficiency in comparison
 1262 with the other regions at $\sim 40^{\circ}\text{S}$ regularly covered by clouds.

1263

1 **Table A1:** Summary of Titan's clouds detected in the complete VIMS dataset between July 2004 and April 2010, classified by flyby (see also
 2 Table 1 in Barnes et al., 2009). For each detections, when available, we indicate the central location of the cloud (in latitudes and eastern
 3 longitudes) and the conditions of observation (mean incidence, emission, phase and spatial resolution). The complete cloud characteristics are
 4 provided for Rodriguez et al. (2009) detections for the T0-T38 time interval (detection maps are available in Rodriguez et al. (2009)
 5 Supplementary Information: <http://www.nature.com/nature/journal/v459/n7247/supinfo/nature08014.html>),
 6 fulfilled by this study up to T67. For T0-T44 time period, the cloud locations are completed with, and compared to, detections of Brown et al.
 7 (2010) (Figure 4).

8 -----

9 ^a SP: cloud detected very near the south pole or at southern high latitudes (poleward of 60°), ~40°S: cloud detected at southern mid-latitudes
 10 (between -60° and -30°), TROP: cloud detected near equator (in a band comprise between -30° and 30°), ~40°N: isolated cloud detected at
 11 northern mid-latitudes (between 30° and 60°), NP: large cloud detected near the North Pole (poleward of 55°).

12

Sequence, Flyby # and date	Cloud type ^a	Avg. central lat.	Avg. central East long.	Mean Inc.	Mean Em.	Mean Phase	Avg. Res. (km)	Observations [R09: Rodriguez et al., 2009] [B10 : Brown et al., 2010]
S02/T0 (1 July 2004)	SP	-66°	-80°	44.5°	42.4°	60.7°	88	One small patch, not centered above the SP. Detected right above the SP by B10 with an extension not seen in the data.
	TROP	-24°	-64°	6.6°	77.4°	76.1°	88	Faint. Detected by B10 10° higher in latitudes and with a more elongated, better shape than that in R09.

	~40°S	-35°	20°		N/A			Very faint. Not detected by R09.
S05/TA (26 Oct. 2004)	SP	-90°		56.3°	67°	14.7°	140	
	~40°S	-56°	-107°	48.3°	61.7°	13.9°	116	
	~40°S	-46°	-92°	53.7°	67.6°	14°	78	
S06/TB (13 Dec. 2004)	SP	-80°	-150°	61°	75.6°	15.7°	47	Large patch very near SP. Detected by B10 with a better shape than R09.
	~40°S	-50°	157°	46.6°	56.4°	15.3°	56	Thin and elongated E-W. Detected by B10 as a large patch too extended in latitudes
	~40°S	-43°	-167°	24.3°	39.4°	17.9°	20	
	~40°S	-49°	-77°	43.7°	54.4°	15.4°	52	
	~40°S	-50°	-130°		N/A			Very faint. Not detected by R09.
	~40°S	-31°	-130°		N/A			Not seen in the data. Detected by B10 almost above the very bright Tui Regio.
S08/T3 (15 Feb. 2005)	NP	60°	all	82.7°	69.9°	14.3°	34	
	SP	-75°	-145°		N/A			Faint. Not detected by R09.
S09/T4 (31 March 2005)	NP	56°	all	78.5°	59.8°	19.1°	85.5	
	SP	-65°	15°	68.1°	70.3°	57°	38	Very near the limb. Not detected by B10.
	SP	-70°	-48°	53.2°	77.3°	57.3°	38	False detection by R09.
	~40°S	-40°	-42°		N/A			Not seen in the data. Detected by B10 as a very small streak.
S10/T5 (16 April 2005)	NP	59°	all	83.8°	63.6°	56.5°	35	
S13/T6	NP	45°	all	67.4°	53.5°	55.5°	74	R09 detect NP cloud at uncertain latitudes (too low).
	SP	-67°	90°		N/A			Faint streak very near the terminator. Not detected by R09.
	~40°S	-58°	20°		N/A			Very faint. Not detected by R09.
S14/T7 (7 Sept. 2005)	NP	59°	all		N/A			Not detected by R09.
	NP	72°	all	94.4°	81.3°	51.5°	62	
S15/T8 (28 Oct. 2005)	SP	-75°	-130°	56.3°	78.6°	24.8°	54	
	NP	73°	all	95.3°	78.4°	22.6°	75	

S17/T9 (26 Dec. 2005)	SP	-76°	45°	60.4°	79.4°	28.5°	83	Small cloud detected above Tui Regio at high phase angle. Not detected by B10.
	TROP	-28°	-119°	66.9°	71°	137.9°	9.8	
	NP	73°	all	94.7°	77.1°	26.6°	70.5	
S17/T10 (15 Jan. 2006)	NP	62°	all	85.7°	79.5°	35.3°	69	
S18/T11 (27 Feb. 2006)	NP	75°	all	98.2°	81.2°	17.3°	93	
S19/T12 (18 March 2006)	~40°S	-38°	-140°		N/A			Extremely faint. Not detected by R09.
	NP	58°	-73°	75.9°	78.3	63.2°	142	
S20/T13 (30 April 2006)								
S20/T14 (20 May 2006)	NP	57°	-90°	76.4°	80.2°	91.2°	106	
S21/T15 (2 July 2006)	~40°S	-45°	25°		N/A			Extremely faint elongated streaks. Not detected by R09. Detected by B10 as a huge complex. Haze artifact?
	NP	62°	60°	79°	79.9°	61°	107	
S22/T16 (22 July 2006)	~40°S	-38°	20°	58.6°	31.5°	59.3°	77	Faint elongated streak. The longitudinal extension seen in the dataset is larger than that of R09, but smaller than that of B10. Not detected by R09.
	NP	57°	all		N/A			
S23/T17 (7 Sept. 2006)	SP	-70°	67°	79.1°	76.4°	55.2°	8.9	Numerous small separated patches and streaks. All detected by B10 as a unique large elongated streak.
	SP	-67°	20°	62.2°	63.9°	58.6°	11.2	
	SP	-62°	42°	70°	57.7°	59.2°	15	
	SP	-75°	-20°		N/A			
	~40°S	-43°	-38°	28.4°	65°	63.8°	52	
	~40°S	-47°	19°	54.5°	42.5°	58.8°	12	
	~40°S	-51°	44°	70.8°	54.7°	54.1°	8	
	~40°S	-45°	45°	73.5°	38.5°	61.9°	36	
	~40°S	-45°	32°	63.3°	40.1°	59°	14	
NP	62°	all	83.9°	78°	63°	65		
S23/T18 (23 Sept. 2006)	NP	55°	all	72.5°	82.5°	64.3°	63	
S24/T19 (9 Oct. 2006)	SP	-76°	all	73.1°	76.3°	64.8°	46	Two distinct elongated streaks. Merged by B10 in a long and large cloud system.
	~40°S	-45°	4°	50.1°	25.2°	64.9°	40	
	~40°S	-44°	32°	67.5°	16.8°	64.6°	44	
	NP	62°	all	79.8°	80.2°	111°	70	

S25/T20 (25 Oct. 2006)	SP	-85°	-85°	70.8°	70.7°	65.3°	12	Numerous small patches near the SP. Merged by B10 in a large cloud system very near the SP.
	SP	-82°	-30°	65.8°	60.8°	65.8°	12	
	SP	-85°	2°	71.2°	61.2°	65.4°	12	
	SP	-77°	-85°	69.6°	71.5°	65.8°	12	
	SP	-78°	22°	67.8°	50.4°	65.3°	12	
	SP	-76°	40°	71.1°	52.5°	65.1°	12	
	SP	-65°	-91°	61.3°	78.9°	67.6°	14	
	SP	-71°	60°	62.3°	74.3°	67.4°	14	
	~40°S	-45°	50°		N/A			Not seen in the data. Detected by B10 as a small patch very near the terminator.
	~40°S	-31°	-48°		N/A			Extremely faint V-shaped streaks. Not detected by R09. Merged by B10 in a large cloud system.
	NP	60°	all	76.3°	80.3°	114°	81	
S26/T21 (12 Dec. 2006)	SP	-85°	-175°			N/A		Not seen in the data. Detected by B10 as a small patch very near the SP.
	SP	-65°	-88°			N/A		Not seen in the data. Detected by B10 as a very large patch extending from ~SP to 50°S latitudes.
	~40°S	-48°	45°	72.6°	15.3°	67.6°	27	System of large and thin streaks. Merged by B10 in a unique huge cloud system. Haze artifact?
	~40°S	-40°	32°	62.9°	10.7°	68.2°	22	
	~40°S	-35°	-40°			N/A		Faint cloud. Not detected by R09.
	TROP	-17°	12°	45.5°	29.9°	68.2°	27	
	TROP	-15°	-17°			N/A		Not seen in the data. Detected by B10 as a small patch.
	NP	65°	all	82.3°	75°	109.2°	89	
S26/T22 (28 Dec. 2006)	SP	-75°	-105°			N/A		Large patch extending up to the SP. Not detected by R09.
	SP	-66°	15°			N/A		Small patch. Not detected by R09.
	~40°S	-40°	30°	55.6°	13.2°	68.7°	15.5	
	~40°S	-35°	-37°			N/A		Not seen in the data. Detected by B10 as a long streak.
	NP	57°	all	74.4°	77.5°	113.8°	90	
S27/T23 (13 Jan. 2007)	SP	-87°	all	77.9°	40°	73.9°	25	
	SP	-64.4°	-54.4°	52.9°	50.9°	74.7°	37	Small patches. Merged by B10 in a huge elongated cloud system too extended in latitudes and longitudes.
	~40°S	-58.9°	-14°	47.8°	35.8°	74.7°	36	
	~40°S	-44°	45°	72.4°	6.1°	74°	27	One elongated streak and small

	~40°S	-47°	17°	54.6°	20.5°	74.6°	41	patches. Merged by B10 in a huge cloud system too extended in latitudes.
	~40°S	-48.5°	-9°	41.2°	35.8°	74.8°	38	
	~40°S	-32°	-20°		N/A			Not seen in the data. Detected by B10 as a large cloud system extending from 45°S up to 5°S with very odd sharp edges. Artifact (borders of a VIMS image).
	NP	55°	All	60.3°	82.4°	110.5°	151	
S27/T24 (29 Jan. 2007)	SP	-80°	-70°	68.9°	47.8°	74.9°	15	Small patches. Merged by B10 in a single cloud system.
	~40°S	-39°	10°	43.2°	34.1°	77°	12.5	Long annular cloud system. Detected by B10 with a better shape than R09.
	NP	56°	All	73.4°	63.5°	105.1°	78	
S28/T25 (22 Feb. 2007)	NP	57°	all	71.8°	17.3°	69.1°	60	
S28/T26 (10 March 2007)	SP	-75°	-175°		N/A			Faint cloud near the SP. Not detected by R09. Detected by B10 as a huge complex too extended in latitudes.
	~40°S	-38°	all		N/A			Faint annular cloud system. Not detected by R09.
	NP	75°	all	87.9°	30.8°	60.8°	29	Small bright patches embedded into a widespread, dimmer, cloud system.
S28/T27 (26 March 2007)	SP	-85°	174°		N/A			Very faint small cloud right above the SP. Not detected by R09.
	SP	-65°	70°		N/A			Very faint small cloud. Not detected by R09.
	SP	-70°	-132°	70.1°	55.1°	125°	45	
	~40°S	-46°	-145°	54.8°	73.4°	123.5°	75	
	TROP	-5°	117°		N/A			Not seen in the data. Detected by B10 as a very small patch.
	NP	62°	all	76.3°	29.8°	52°	65	Small bright patches embedded into a widespread, dimmer, cloud system.
S29/T28 (10 April 2007)	SP	-88°	all		N/A			Very faint small cloud right above the SP. Not detected by R09.
	~40°S	-45°	-134°	62.5°	78.5°	130.8°	69	Elongated streak and small patches. Detected by B10 as a huge complex that expands too far in the south.
	NP	55°	all	69.4°	29.7°	45.1°	35	Small bright patches embedded into a widespread, dimmer, cloud system.

S29/T29 (26 April 2007)	SP	-73°	all	62.5°	78.5°	139.5°	96	Very faint small cloud. Not detected by R09.
	TROP	-5°	130°	N/A				
	NP	56°	all	71.1°	38.5°	36.5°	76	
S30/T30 (12 May 2007)	SP	-63°	-118°	52.7°	79.8°	144°	92	Small bright patches embedded into a widespread, dimmer, cloud system. Cloud detected by R09 near the limb. Uncertain. Data not used by B10.
	~40°S	-56°	130°	50.5°	76.5°	29.8°	83.5	
	NP	57°	all	73.4°	49.3°	28.7°	73	
S30/T31 (28 May 2007)	~40°S	-51°	110°	58.6°	75.7°	25.1°	61	
	~40°S	-52°	127°	55.5°	73.7°	25.1°	62	
	NP	65.5°	all	85.9°	67.7°	23.6°	56	
S31/T32 (13 June 2007)	SP	-73°	all	62.8°	77.9°	16°	76	Annular cloud system. Detected by B10 with a better shape than R09.
	~40°S	-53°	-158°	60°	75.5°	15.6°	65	
	~40°S	-47°	80°	70.7°	76.8°	15.5°	113	
	NP	66.5°	all	88.7°	75.9°	14.8°	98	
S31/T33 (29 June 2007)	~40°S	-48°	100°	55.4°	64.8°	16.9°	18	Very thin streaks and small patches. Merged by B10 in a larger cloud system with an odd shape.
	~40°S	-50°	118°	49.6°	59.6°	16°	18	
	~40°S	-45°	-178°	48.3°	59.3°	12.3°	118	
	NP	71°	All	83.9°	73.7°	11.9°	91	
S32/T34 (19 July 2007)	~40°S	-46°	150°	59.5°	75.6°	124.2°	112	Thin streaks and small patches. Merged by B10 in a larger and longer cloud system. Not seen in the data. Detected by B10 as a very small patch. Not seen in the data. Detected by B10 as a very small and thin streak.
	~40°S	-42°	17°	66.7°	45.3°	55.8°	18	
	~40°S	-45°	32°	52.1°	46.9°	59.6°	50	
	TROP	-25°	175°	N/A				
	TROP	-10°	150°	N/A				
S33/T35 (31 Aug. 2007)	NP	62.5°	All	74°	79.7°	61.4°	129	
	NP	60°	All	75.5°	65.3°	27.7°	28	
S34/T36 (2 Oct. 2007)	~40°S	-53°	110°	70.3°	65.3°	32.6°	82	Faint elongated patches. Detected by B10 as an almost complete annular belt at ~40°S, with a larger latitudinal extension than seen in the data. Not seen in the data. Detected by B10 as a very small patch.
	~40°S	-46°	-144°	50.2°	78.6°	33°	68	
	TROP	-10°	150°	N/A				
	NP	58.5°	all	77.1°	79.4°	32.6°	92	
S35/T37 (19 Nov. 2007)	~40°S	-50°	-160°	N/A				Very faint and small patch, right at the terminator. Uncertain. Not detected by R09.

	NP	70°	all	81.6°	76.9°	41.2°	120	
S35/T38 (5 Dec. 2007)	SP	-66°	-100°	72.3°	77.3°	137°	16	Long streak detected at high phase angle near the limb. Not detected by B10.
	~40°S	-50°	115°		N/A			Very faint, but large cloud. Not as large as detected by B10. Not detected by R09.
	NP	60°	all	76.6°	76.2°	44.9°	142	
S36/T39 (20 Dec. 2007)	~40°S	-49°	-85°	74.3°	62.4°	134°	86	
	NP	71°	all	82.8°	58.4°	50°	102	
S36/T40 (5 Jan. 2008)	SP	-68°	-100°		N/A			Not seen in the data. Detected by B10 at very high phase angle as very thin and small patches.
	~40°S	-45°	-85°		N/A			
	TROP	-16°	-92°		N/A			
S38/T41 (22 Feb. 2008)	NP	60°	all	77.3°	69.1°	57.5°	66	
	TROP	-26°	-98°	62.5°	57.5°	119.5°	69	
S39/T42 (26 March 2008)	NP	69°	all	81.5°	53.5°	65.7°	71	
	SP	-77°	-160°	69.2°	69.1°	109.6°	15	Not seen in the data. Detected by B10 at very high phase angle as a large streak.
	~40°S	-50°	-125°		N/A			
	~40°S	-37°	-80°		N/A			Not seen in the data. Detected by B10 at very high phase angle as very small patches.
	TROP	-25°	-115°	47.3°	72.8°	111.7°	98	
	TROP	-22°	-80°	80.9°	32.1°	110.2°	21	Thin streaks and patches. All merged by B10 in a larger cloud system. Haze artifact?
	TROP	-25°	-80°	80.8°	31.5°	110.1°	21	
	TROP	-17°	-72°	88.6°	24.3°	110°	22	
NP	66°	All	76.7°	58.3°	73.6°	99		
S40/T43 (12 May 2008)	SP	-80°	-110°		N/A			Not seen in the data. Detected by B10 as very small patches very near the SP.
	SP	-67°	-172°	61.2°	75.3°	102.6°	79	
	~40°S	-37°	-125°	41.8°	63.6°	103°	84	Small patches. All merged by B10 in a larger cloud system too extended in latitudes and longitudes. Haze artifact?
	~40°S	-40°	-90°		N/A			Not seen in the data. Detected by B10 as small patches.
	TROP	-11°	-105°	51.2°	56.9°	102.8°	74	
S40/T44 (28 May 2008)	NP	66°	All	74.7	58.4°	82.1°	83	
	SP	-81°	-41°	87.6°	54.9°	94°	48	Small patch. Not detected by B10.
	SP	-80°	-98°	79.2°	55.4°	94.3°	54	Large patch. Not detected by B10.

	~40°S	-41°	-93°	63.8°	34.8°	95.7°	100	Small patch. Not detected by B10.
	~40°S	-44°	134°	61.7°	77.4°	89.2°	42	Large patch. Not detected by B10.
	TROP	-16°	-93°	65.5°	30.9°	93.5°	33	Small patches. Not detected by B10.
	NP	81°	all	89.8°	63.3°	88.5°	64	One central cap encircled by an annular faint cloud. All merged by B10 in a larger cloud system too extended southward in latitudes (down to 35°N). Haze artifact?
	NP	62°	all	75.5°	51.8°	88.9°	71	
S42/T45 (31 July 2008)	SP	-88°	all	84.4°	64.6°	86.4°	136	
	NP	74°	all	84.8°	59.3°	96.8°	75	
S45/T46 (3 Nov. 2008)	~40°S	-37°	-159°	35.7°	72°	81.6°	64	One central cap encircled by an annular faint cloud.
	NP	62°	all	71.7°	52°	94.8°	110	
	NP	83°	all	89.3°	58.4°	94.5°	112	
S45/T47 (19 Nov. 2008)	NP	61°	all	70.9°	63.5°	100.3°	97	One central cap encircled by an annular faint cloud.
	NP	83°	all	88°	58.2°	100.2°	113	
S46/T48 (5 Dec. 2008)	SP	-77°	146°	81.4°	64.9°	77.3°	79	One central cap encircled by an annular faint cloud.
	~40°S	-41°	171°	48.5°	80.3°	76.1°	23	
	NP	64°	all	75.3°	55.8°	108.3°	112	
	NP	82°	all	87.5°	54.5°	108.2°	116	
S46/T49 (21 Dec. 2008)	~40°S	-42°	-119°	46.4°	29.2°	71.2°	51	One central cap encircled by an annular faint cloud.
	~40°S	-40°	-100°	60.6°	10.6°	70.8°	18	
	~40°S	-34°	-92°	64°	10.5°	70.5°	15	
	TROP	-12°	-133°	21.1°	52.6°	72.4°	29	
	NP	73°	all	81.3°	50°	110.3°	96	
S47/T50 (7 Feb. 2009)	NP	66°	all	76.5°	47.1°	105.9°	97	Faint annular cloud.
S49/T51 (27 March 2009)	~40°S	-49°	-157°	47.6°	44.4°	75.2°	65	One central cap encircled by an annular faint cloud.
	~40°S	-47°	-68°	80.6°	10.7°	74.5°	49	
	NP	65°	all	75.3°	43.7°	106.2°	99	
	NP	83°	all	86.7°	35.2°	106.1°	114	
S49/T52 (4 April 2009)	~40°S	-49°	-21°	57.6°	53.1°	73.8°	59	
	~40°S	-52°	28°	52.8°	39.1	74.1°	59	
	~40°S	-46°	47°	66.4°	50.1°	71.9°	100	
	NP	67°	all	77.3°	42.7°	108.3°	83	
S49/T53 (20 April 2009)	~40°S	-42°	12°	52.4°	52.4°	67.6°	83	
	NP	70°	all	78.6°	36.3°	80.2°	368	
S50/T54 (5 May 2009)	NP	80°	70°	82.7°	45.3°	118.7°	57	Patchy.
S50/T55	~40°S	-42°	-7°	50.5°	37.3°	52.3°	137	

(21 May 2009)	~40°S	-42°	30°	48.5°	35.4°	52°	157	One central cap encircled by an annular faint cloud.
	~40°S	-43°	70°	55°	12.8°	54.6°	37	
	TROP	-25°	73°	48°	30.9°	55.2°	34	
	NP	80°	All	84.5°	41.8°	121.3°	125	
S50/T56 (6 June 2009)	~40°S	-44°	41°	52°	20.7°	44.2°	111	Large diffuse patch very near the equator. Patchy.
	~40°S	-43°	-34°	62.8°	46.9°	44.1°	111	
	TROP	-26°	-20°	48.9°	49.7°	44.4°	110	
	TROP	-3°	19°	8.8°	43.5°	44.3°	131	
S51/T57 (22 June 2009)	NP	71°	57°	72.5°	61.3°	130.2°	82	Patchy.
	~40°S	-39°	-21°	50.9°	29.8°	36.3°	81	
	~40°S	-40°	24°	49°	21.8°	36.5°	71	
	~40°S	-38°	78°	55.8°	29.7°	36.4°	71	
	~40°S	-52°	96°	75.4°	44.5°	36.1°	67	
S51/T58 (8 July 2009)	NP	79°	36°	80.3°	59.3°	138.6°	76	Patchy.
	~40°S	-52°	-22°	68.3°	48.2°	28.4°	49	
	~40°S	-44°	-7°	54.3°	33.9°	28.2°	67	
	~40°S	-43°	72°	53.1°	28.8°	30.3°	30	
	~40°S	-44°	102°	75.7°	55.4°	28.7°	41	
S52/T59 (24 July 2009)	NP	79°	40°	80.3°	68.1°	148.1°	52	Patchy.
S52/T60 (9 Aug. 2009)								
S53/T61 (25 Aug. 2009)	~40°S	-45°	50°	47°	42.9°	11.1°	24	
	~40°S	-46°	14°	50.4°	41°	11.8°	52	
S54/T62 (12 Oct. 2009)	~40°S	-44°	33°	46.5°	45.3°	10.9°	57	Patchy.
	~40°S	-44°	-12°	60.9°	53.6°	10.2°	61	
	~40°N	31°	-6°	43.3°	39.7°	10.4°	98	
	~40°N	31°	4°	43.5°	39.5°	10.4°	98	
	NP	69°	50°	69.5°	73.9°	10.8°	103	
S55/T63 (12 Dec. 2009)	~40°S	-47°	140°	60°	53.7°	48.1°	47	Huge system, also constituted of some small patches and E-W elongated streaks. Patchy.
	~40°S	-40°	162°	65.7°	44.4°	48.5°	33	
	~40°N	46°	-176°	82.3°	56.6°	46.1°	56	
	~40°N	47°	178°	76.3°	53.1°	46.2°	57	
	NP	71°	-120°	77°	76°	45.7°	86	
S56/T64 (28 Dec. 2009)	~40°S	-52°	-178°	81.2°	53.1°	42.8°	36	Patchy.
	~40°S	-50°	70°	52.7°	59.6°	48.1°	386	
	NP	68°	160°	72.6°	79.6°	44.6°	75	
S56/T65 (12 Jan. 2010)	~40°S	-50°	172°	69.5°	49°	43.2°	50	
	~40°S	-52°	150°	65.7°	48.1°	43.3°	56	
	TROP	-14°	90°	22.6°	58.9°	44.4°	62	

	NP	68°	150°	74.5°	75.2°	43.8°	124	Patchy.
S57/T66 (28 Jan. 2010)	~40°S	-54°	89°	59.7°	62.1°	38.6°	16	
	~40°S	-53°	61°	68.7°	78.9°	39.2°	17	
	~40°S	-58°	148°	71.2°	56.1°	43.1°	75	
	~40°S	-49°	169°	79.5°	53°	42.3°	63	
	~40°S	-45°	165°	78.7°	49.7°	42.6°	69	
	~40°S	-44°	81°	54.8°	52.5°	38.1°	9	
	~40°S	-34°	89°	42.2°	53.2°	39.1°	12	
	NP	69°	150°	75.6°	75.5°	44.3°	124	
								Patchy.
S59/T67 (5 April 2010)	NP	74°	10°	74.1°	78.3°	16.4°	94	Patchy.

13